Elsevier Editorial System(tm) for Journal of Colloid and Interface Science
Manuscript Draft

Manuscript Number: JCIS-13-2404R1

Title: EARLY IN VITRO RESPONSE OF MACROPHAGES AND T LYMPHOCYTES TO NANOCRYSTALLINE HYDROXYAPATITES

Article Type: Regular Article

Section/Category: E. Biomaterials and Nanomedicine

Keywords: biocompatibility; cytokine; hydroxyapatite; lymphocyte; macrophage.

Corresponding Author: Prof. M.Teresa Portolés, Professor, PhD

Corresponding Author's Institution: Faculty of Chemistry, Universidad Complutense

First Author: María Concepción Matesanz

Order of Authors: María Concepción Matesanz; María José Feito, PhD; Mercedes Oñaderra, Professor, PhD; Cecilia Ramírez-Santillán; Carmen da Casa; Daniel Arcos, PhD; María Vallet-Regí, Professor, PhD; José María Rojo, PhD; M.Teresa Portolés, Professor, PhD

Abstract: Hypothesis
Synthetic hydroxyapatite (HA) and Si substituted hydroxyapatite (SiHA) are calcium phosphate ceramics currently used in the field of dentistry and orthopaedic surgery. The preparation of both biomaterials as polycrystalline solid pieces or grains formed by nanocrystallites has awakened a great interest to enhance the bioactive behavior due to the microstructural defects and the higher surface area. The study of the macrophage and lymphocyte behavior in contact with nanocrystalline HA and SiHA will allow to elucidate the immune response which conditions the success or rejection of these biomaterials.
Experiments
HA and SiHA granules (with sizes of tens of microns) have been prepared by controlled aqueous precipitation avoiding subsequent high temperature sintering. HA and SiHA granules were constituted by crystallites smaller than 50 nm. The effects of both nanocrystalline materials on immune system have been evaluated with macrophages (main components of innate immune system) and T lymphocytes (specific cells of adaptive response) after short-term culture as in vitro models of the early immune response.
Findings
Significant decreases of macrophage proliferation and phagocytic activity, increased production of inflammatory cytokines (IL-6, TNF-alpha) and T lymphocyte apoptosis, were induced by these nanocrystalline ceramics suggesting that, after in vivo implantation, they induce significant effects on immune responses, including an early activation of the innate immune system.

Madrid, October 23, 2013

Dear Editor:

Concerning our revised manuscript entitled "EARLY IN VITRO RESPONSE OF MACROPHAGES AND T LYMPHOCYTES TO NANOCRYSTALLINE HYDROXYAPATITES" (your reference: JCIS-13-2404), we have taken the Reviewers´ comments into account and I am glad to send you the revised version of the manuscript which includes all the changes made **marked in blue**. The authors thank the comments of the reviewers aimed to improve the quality of our manuscript. A detailed list of these changes and the responses to the Reviewers' comments is included below.

Reviewer #1:

1- The authors have produced a logical and straightforward ms highlighting an important topic. The presented work is of good quality. However, the ms could be improved if the authors considered experiments aimed at adding some physiological importance. Effects of human plasma as well as saliva adsorption to HA particles could be evaluated (TNF, phagocytosis etc). Human monocytes (purified from blood), or the THP-1 cell line could be tested in order to show physiological relevance. Not all conditions need to be tested, but would be valuable if the authors could show some conceptual data in human systems.

Authors

Concerning the possible effect of HA particles in human systems, previous experiments were carried out with human Saos-2 osteoblasts cultured for 4 days in the presence of 1 mg/ml of either nanocrystalline hydroxyapatite (nano-HA) or silicon-doped hydroxyapatite (nano-SiHA). Saos-2 osteoblasts proliferated in contact with both materials, but the cell number was significantly lower than in controls. However, the number of Saos-2 cells in contact with nano-SiHA was significantly higher than with nano-HA, indicating that this cell type grows better in the presence of nano-SiHA. This result was also observed by Scanning Electron Microscopy (SEM) when Saos-2 osteoblasts were cultured for 4 days on surface of both nano-HA and nano-SiHA disks. SEM images demonstrated that Saos-2 cells adhere to the nano-SiHA disks, proliferate and colonize their surface better than on HA disks. Although low levels of apoptosis were obtained in human Saos-2 osteoblasts after contact with these materials, this cell type showed a slight increase of cell apoptosis in the presence of nano-HA (2.1 %) in comparison to nano-SiHA (0.4%) and control cells (0.3%). Intracellular ROS content did not show alteration in the presence of these materials, thus indicating no oxidative stress (reference 11). Comments on these previous results with human Saos-2 osteoblasts have been included in the revised version of the manuscript (pages 11 and 12).

2- I also wonder about the specificity of the response. Could other biomaterials, polymers etc generate the same results? Thus, is the observed activation characteristic for HA? The authors should discuss this.

Authors

Concerning the effects of other biomaterials as polymers etc, previous results demonstrate different cellular responses depending on each biomaterial and depending on each cell type. For example, biocompatibility studies with poly(ε-caprolactone) (PCL) and L929 fibroblasts have shown that, although cells proliferate significantly slower on PCL films than on control surface during the first 48 h in culture, this effect disappears after 3 days treatment, showing a significant stimulation of the cell proliferation on the PCL films at longer culture times (ref 37: Serrano MC, Pagani R, Vallet-Regí M, Peña J, Rámila A, Izquierdo I, Portolés MT. In vitro biocompatibility assessment of poly(ε-caprolactone) films using L929 mouse fibroblast. Biomaterials 2004;25:5603-5611). Previous biocompatibility studies with mesostructured bioactive glasses (MBGs) showed satisfactory results but a cytostatic effect was observed through the reduction of cell proliferation (ref 38: Alcaide M, Portolés P, López-Noriega A, Arcos D, Vallet-Regí M, Portolés MT. Interaction of an ordered mesoporous bioactive glass with osteoblasts, fibroblasts and lymphocytes demonstrates its biocompatibility as a potential bone graft material. Acta Biomaterialia 2010;6:892-899). However, high proliferation values were obtained with a mesostructured nanocomposite formed by nanocrystalline apatite particles uniformly embedded into MBG (ref 39: Cicuéndez M, Portolés MT, Izquierdo-Barba I, Vallet-Regí M. New nanocomposite system with nanocrystalline apatite embedded into mesoporous bioactive glass. Chemistry of Materials 2012;24:1100-1106). In conclusion, the effects observed in the present study with nano-HA and nano-SiHA on macrophages and lymphocytes are characteristic for these materials and for the cell types used in this study. All these references (37-39) and a comment concerning the cell type and material dependent response in biocompatibility studies have been included in the revised version of the manuscript (pages 14 and 15).

3- Minor comments: Bar diagrams are not effective, and could be compressed in order to save space.

Authors

The bar diagrams have been compressed in figures 3, 5, 7, 8, 9, and 10 in order to save space, as suggested by the reviewer.

Reviewer #2:

1- The fluorescence intensity in Fig. 5B gives an indication of the extent of phagocytosis. For fresh murine macrophages and nano-SiHA, a decrease in cell proliferation resulted in decreased fluorescence, which is expected since there are fewer cells to take in the FTIC-functionalized latex beads. Similar results were shown in Fig. 3 for the RAW macrophages. But for fresh murine macrophages and nano-HA, while the cell proliferation decreased, the fluorescence is unaffected (Fig. 5A). Some explanations should be provided for this unexpected result.

Authors

Figures 3B and 5B show the effects of nano-HA and nano-SiHA on phagocytosis of RAW and murine fresh macrophages respectively. In these flow cytometry studies, 10,000 cells were analyzed in each sample and the mean of the fluorescence emitted by these 10,000 cells of each sample was used. Thus, the fluorescence indicates the phagocytic activity of these 10,000 cells and it is not dependent on the number of cells obtained in cell proliferation studies. On the other hand, the different effect of nano-HA on RAW and fresh macrophages can be due to the higher values of phagocytosis obtained with fresh macrophages which always showed higher fluorescence values (Figure 5B) than RAW macrophages (Figure 3B). This fact can be associated with a lower sensitivity to nano-HA of fresh macrophages although the phagocytic activity of these cells was affected by nano-SiHA. More details concerning the effects of these materials on phagocytosis are included in the revised manuscript (page 12).

2- Nano-SiHA and nano-HA seemed to have less adverse effects on RAW macrophage proliferation than on fresh murine macrophage proliferation. Why is this so? From Table III, it appears that ROS production in RAW macrophages was not significantly affected. Is this conclusion the same for fresh murine macrophages?

Authors

As it has been indicated above, different cellular responses are obtained depending on each biomaterial and depending on each cell type (references 37-39). RAW 264.7 cells are functional macrophages with the ability of autophagy and phagocytosis as immune cells and retain many of the characteristics of macrophages in vivo, for these reasons this cell line is usually used for in vitro biocompatibility studies. However, fresh murine macrophages are primary cells and their proliferation rate is slower than with RAW cells.

3- The bioassays were all done after 3 days of incubation. Some experiments should be carried out to show the time dependence of the effects of the nano-SiHA and nano-HA on the cells, say 1 day.

Authors

The authors thank the suggestion of the reviewer. Assays after 1 day of incubation and long-term studies are currently being carried out to know the time dependence and to identify macrophage activation markers for determine the effects of these materials on M1 and M2 phenotypes.

4- Fig. 9 shows that lymphocyte proliferation and viability were not affected by nano-SiHA and nano-HA, but since these materials produce an increase in apoptosis, why is the cell viability and proliferation not affected?

Authors

Cell viability was determined by 0.2% Trypan Blue exclusion which indicates the integrity of plasma membrane. Apoptosis was determined by SubG1 fraction which corresponds to cells with fragmented DNA. After culture in the presence of nano-HA and nano-SIHA, some cells can be with damaged plasma membrane but without apoptosis. Thus, necrotic

cells are usually defined by the lack of integrity of the plasma membrane. In contrast, apoptotic cells have an intact plasma membrane. For this reason, both parameters (cell viability and apoptosis) are independent and evaluated through different techniques. Although these materials induce lymphocyte apoptosis, proliferation is not affected probably due to the hyperreactivity of SR.D10 lymphocytes, as it is indicated in the manuscript (page 14).

I do hope you will consider the reviewed manuscript suitable for publication.

Thanking you very much for your attention, I remain

Sincerely yours

Prof. M. Teresa Portolés
Departamento de Bioquímica y Biología Molecular I
Facultad de Ciencias Químicas
Universidad Complutense, 28040-Madrid, Spain
E-mail: portoles@quim.ucm.es

Madrid, October 23, 2013

Dear Editor:

Concerning our revised manuscript entitled "EARLY IN VITRO RESPONSE OF MACROPHAGES AND T LYMPHOCYTES TO NANOCRYSTALLINE HYDROXYAPATITES" (your reference: JCIS-13-2404), we have taken the Reviewers´ comments into account and I am glad to send you the revised version of the manuscript which includes all the changes made **marked in blue**. The authors thank the comments of the reviewers aimed to improve the quality of our manuscript. A detailed list of these changes and the responses to the Reviewers' comments is included below.

Reviewer #1:

1- The authors have produced a logical and straightforward ms highlighting an important topic. The presented work is of good quality. However, the ms could be improved if the authors considered experiments aimed at adding some physiological importance. Effects of human plasma as well as saliva adsorption to HA particles could be evaluated (TNF, phagocytosis etc). Human monocytes (purified from blood), or the THP-1 cell line could be tested in order to show physiological relevance. Not all conditions need to be tested, but would be valuable if the authors could show some conceptual data in human systems.

Authors

Concerning the possible effect of HA particles in human systems, previous experiments were carried out with human Saos-2 osteoblasts cultured for 4 days in the presence of 1 mg/ml of either nanocrystalline hydroxyapatite (nano-HA) or silicon-doped hydroxyapatite (nano-SiHA). Saos-2 osteoblasts proliferated in contact with both materials, but the cell number was significantly lower than in controls. However, the number of Saos-2 cells in contact with nano-SiHA was significantly higher than with nano-HA, indicating that this cell type grows better in the presence of nano-SiHA. This result was also observed by Scanning Electron Microscopy (SEM) when Saos-2 osteoblasts were cultured for 4 days on surface of both nano-HA and nano-SiHA disks. SEM images demonstrated that Saos-2 cells adhere to the nano-SiHA disks, proliferate and colonize their surface better than on HA disks. Although low levels of apoptosis were obtained in human Saos-2 osteoblasts after contact with these materials, this cell type showed a slight increase of cell apoptosis in the presence of nano-HA (2.1 %) in comparison to nano-SiHA (0.4%) and control cells (0.3%). Intracellular ROS content did not show alteration in the presence of these materials, thus indicating no oxidative stress (reference 11). Comments on these previous results with human Saos-2 osteoblasts have been included in the revised version of the manuscript (pages 11 and 12).

2- I also wonder about the specificity of the response. Could other biomaterials, polymers etc generate the same results? Thus, is the observed activation characteristic for HA? The authors should discuss this.

Authors

Concerning the effects of other biomaterials as polymers etc, previous results demonstrate different cellular responses depending on each biomaterial and depending on each cell type. For example, biocompatibility studies with poly(ε-caprolactone) (PCL) and L929 fibroblasts have shown that, although cells proliferate significantly slower on PCL films than on control surface during the first 48 h in culture, this effect disappears after 3 days treatment, showing a significant stimulation of the cell proliferation on the PCL films at longer culture times (ref 37: Serrano MC, Pagani R, Vallet-Regí M, Peña J, Rámila A, Izquierdo I, Portolés MT. In vitro biocompatibility assessment of poly(ε-caprolactone) films using L929 mouse fibroblast. Biomaterials 2004;25:5603-5611). Previous biocompatibility studies with mesostructured bioactive glasses (MBGs) showed satisfactory results but a cytostatic effect was observed through the reduction of cell proliferation (ref 38: Alcaide M, Portolés P, López-Noriega A, Arcos D, Vallet-Regí M, Portolés MT. Interaction of an ordered mesoporous bioactive glass with osteoblasts, fibroblasts and lymphocytes demonstrates its biocompatibility as a potential bone graft material. Acta Biomaterialia 2010;6:892-899). However, high proliferation values were obtained with a mesostructured nanocomposite formed by nanocrystalline apatite particles uniformly embedded into MBG (ref 39: Cicuéndez M, Portolés MT, Izquierdo-Barba I, Vallet-Regí M. New nanocomposite system with nanocrystalline apatite embedded into mesoporous bioactive glass. Chemistry of Materials 2012;24:1100-1106). In conclusion, the effects observed in the present study with nano-HA and nano-SiHA on macrophages and lymphocytes are characteristic for these materials and for the cell types used in this study. All these references (37-39) and a comment concerning the cell type and material dependent response in biocompatibility studies have been included in the revised version of the manuscript (pages 14 and 15).

3- Minor comments: Bar diagrams are not effective, and could be compressed in order to save space.

Authors

The bar diagrams have been compressed in figures 3, 5, 7, 8, 9, and 10 in order to save space, as suggested by the reviewer.

Reviewer #2:

1- The fluorescence intensity in Fig. 5B gives an indication of the extent of phagocytosis. For fresh murine macrophages and nano-SiHA, a decrease in cell proliferation resulted in decreased fluorescence, which is expected since there are fewer cells to take in the FTIC-functionalized latex beads. Similar results were shown in Fig. 3 for the RAW macrophages. But for fresh murine macrophages and nano-HA, while the cell proliferation decreased, the fluorescence is unaffected (Fig. 5A). Some explanations should be provided for this unexpected result.

Authors

Figures 3B and 5B show the effects of nano-HA and nano-SiHA on phagocytosis of RAW and murine fresh macrophages respectively. In these flow cytometry studies, 10,000 cells were analyzed in each sample and the mean of the fluorescence emitted by these 10,000 cells of each sample was used. Thus, the fluorescence indicates the phagocytic activity of these 10,000 cells and it is not dependent on the number of cells obtained in cell proliferation studies. On the other hand, the different effect of nano-HA on RAW and fresh macrophages can be due to the higher values of phagocytosis obtained with fresh macrophages which always showed higher fluorescence values (Figure 5B) than RAW macrophages (Figure 3B). This fact can be associated with a lower sensitivity to nano-HA of fresh macrophages although the phagocytic activity of these cells was affected by nano-SiHA. More details concerning the effects of these materials on phagocytosis are included in the revised manuscript (page 12).

2- Nano-SiHA and nano-HA seemed to have less adverse effects on RAW macrophage proliferation than on fresh murine macrophage proliferation. Why is this so? From Table III, it appears that ROS production in RAW macrophages was not significantly affected. Is this conclusion the same for fresh murine macrophages?

Authors

As it has been indicated above, different cellular responses are obtained depending on each biomaterial and depending on each cell type (references 37-39). RAW 264.7 cells are functional macrophages with the ability of autophagy and phagocytosis as immune cells and retain many of the characteristics of macrophages in vivo, for these reasons this cell line is usually used for in vitro biocompatibility studies. However, fresh murine macrophages are primary cells and their proliferation rate is slower than with RAW cells.

3- The bioassays were all done after 3 days of incubation. Some experiments should be carried out to show the time dependence of the effects of the nano-SiHA and nano-HA on the cells, say 1 day.

Authors

The authors thank the suggestion of the reviewer. Assays after 1 day of incubation and long-term studies are currently being carried out to know the time dependence and to identify macrophage activation markers for determine the effects of these materials on M1 and M2 phenotypes.

4- Fig. 9 shows that lymphocyte proliferation and viability were not affected by nano-SiHA and nano-HA, but since these materials produce an increase in apoptosis, why is the cell viability and proliferation not affected?

Authors

Cell viability was determined by 0.2% Trypan Blue exclusion which indicates the integrity of plasma membrane. Apoptosis was determined by SubG1 fraction which corresponds to cells with fragmented DNA. After culture in the presence of nano-HA and nano-SIHA, some cells can be with damaged plasma membrane but without apoptosis. Thus, necrotic

cells are usually defined by the lack of integrity of the plasma membrane. In contrast, apoptotic cells have an intact plasma membrane. For this reason, both parameters (cell viability and apoptosis) are independent and evaluated through different techniques. Although these materials induce lymphocyte apoptosis, proliferation is not affected probably due to the hyperreactivity of SR.D10 lymphocytes, as it is indicated in the manuscript (page 14).

I do hope you will consider the reviewed manuscript suitable for publication.

Thanking you very much for your attention, I remain

Sincerely yours

Prof. M. Teresa Portolés
Departamento de Bioquímica y Biología Molecular I
Facultad de Ciencias Químicas
Universidad Complutense, 28040-Madrid, Spain
E-mail: portoles@quim.ucm.es

*3: Graphical Abstract (for review)

Click here to download high resolution image

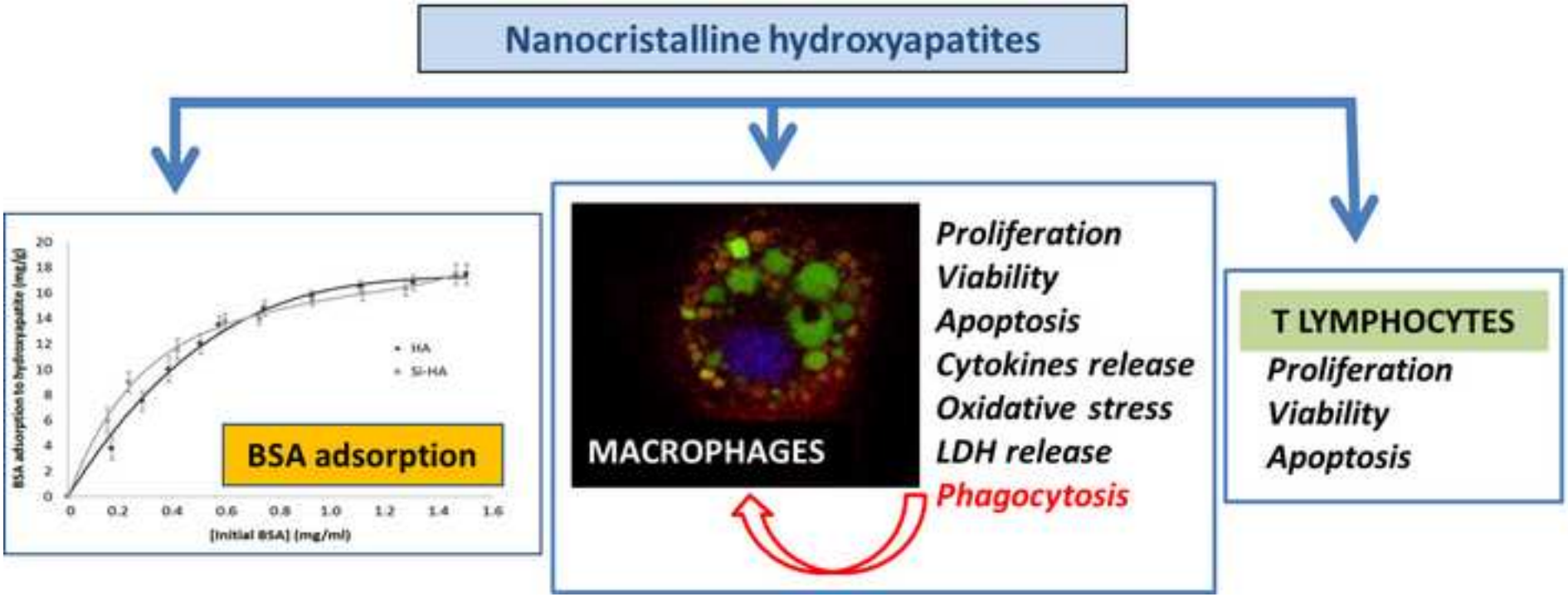

Highlights

- Macrophage/lymphocyte response to nanocrystalline hydroxyapatites was evaluated
- Nanocrystalline hydroxyapatites decreased macrophage proliferation and phagocytosis
- Increased production of inflammatory cytokines IL-6 and TNF-α was detected
- T lymphocyte apoptosis was increased without proliferation changes
- Nanocrystalline hydroxyapatites might induce early immune system activation

EARLY *IN VITRO* RESPONSE OF MACROPHAGES AND T LYMPHOCYTES TO NANOCRYSTALLINE HYDROXYAPATITES

María Concepción Matesanz[a], María José Feito[a], Mercedes Oñaderra[a], Cecilia Ramírez-Santillán[a], Carmen da Casa[a], Daniel Arcos[b,c], María Vallet-Regí[b,c], José María Rojo[d], María Teresa Portolés [a*]

[a]Department of Biochemistry and Molecular Biology I, Faculty of Chemistry, Universidad Complutense, 28040-Madrid, Spain

conchitamatesanz@hotmail.com, mjfeito@pdi.ucm.es, monaderr@bio.ucm.es, cecilia27884@hotmail.com, cdacasa_19991@hotmail.com, portoles@quim.ucm.es

[b]Department of Inorganic and Bioinorganic Chemistry, Faculty of Pharmacy, UCM, Instituto de Investigación Sanitaria Hospital 12 de Octubre i+12, 28040-Madrid, Spain

arcosd@farm.ucm.es, vallet@farm.ucm.es

[c]Networking Research Center on Bioengineering, Biomaterials and Nanomedicine, CIBER-BBN, Spain

[d]Department of Cellular and Molecular Medicine, Centro de Investigaciones Biológicas, CSIC, 28040-Madrid, Spain

jmrojo@cib.csic.es

* Corresponding author: Prof. María Teresa Portolés. Departamento de Bioquímica y Biología Molecular I, Facultad de Ciencias Químicas, Universidad Complutense, 28040-Madrid, Spain. Telephone: 34-1-394 46 66, Fax: 34-1-394 41 59, E-mail: portoles@quim.ucm.es

Abstract

Hypothesis

Synthetic hydroxyapatite (HA) and Si substituted hydroxyapatite (SiHA) are calcium phosphate ceramics currently used in the field of dentistry and orthopaedic surgery. The preparation of both biomaterials as polycrystalline solid pieces or grains formed by nanocrystallites has awakened a great interest to enhance the bioactive behavior due to the microstructural defects and the higher surface area. The study of the macrophage and lymphocyte behavior in contact with nanocrystalline HA and SiHA will allow to elucidate the immune response which conditions the success or rejection of these biomaterials.

Experiments

HA and SiHA granules (with sizes of tens of microns) have been prepared by controlled aqueous precipitation avoiding subsequent high temperature sintering. HA and SiHA granules were constituted by crystallites smaller than 50 nm. The effects of both nanocrystalline materials on immune system have been evaluated with macrophages (main components of innate immune system) and T lymphocytes (specific cells of adaptive response) after short-term culture as *in vitro* models of the early immune response.

Findings

Significant decreases of macrophage proliferation and phagocytic activity, increased production of inflammatory cytokines (IL-6, TNF-α) and T lymphocyte apoptosis, were induced by these nanocrystalline ceramics suggesting that, after *in vivo* implantation, they induce significant effects on immune responses, including an early activation of the innate immune system.

Keywords: biocompatibility, cytokine, hydroxyapatite, lymphocyte, macrophage.

1. Introduction

Immediately after biomaterial-tissue contact, blood and interstitial fluid proteins adsorb to the biomaterial surface and activate the coagulation cascade, complement system, platelets and immune cells [1,2]. Thus, the evaluation of serum proteins adsorption and the biomaterial effects on immune system are essential aspects of biocompatibility assessment [3,4]. The immune response comprises both innate and adaptive defence mechanisms which co-ordinately activate different cell populations. Neutrophils, monocytes and macrophages are critical cellular components of the innate immune response, carrying out phagocytosis and producing reactive oxygen species, antimicrobial peptides, and inflammatory mediators [5]. The adaptive response is mediated by antigen-specific lymphocytes (T and B cells) and by their products, which include inflammatory cytokines and antibodies. Although the interaction of immune cells with biomaterials has been considered negative for a long time, specific cell responses may be beneficial for biomaterial integration and improve implant performance [6]. Recent studies demonstrate the potential of biomaterials to modulate immune cell function suggesting the possibility of designing biomaterials capable of eliciting appropriate immune responses at implantation sites [7].

Because of its similarity to the mineral component of bone, synthetic hydroxyapatite (HA) is a calcium phosphate ceramic widely used in the field of dentistry and orthopaedic surgery with different purposes. Its main applications are grafting for small bone defects, coatings of metallic prostheses and periodontal implants, and as scaffolds for bone tissue engineering [8]. Silicon substituted hydroxyapatites (SiHAs) have attracted the attention of many researchers [9-13] and have recently been incorporated to the biomaterials market as Actifuse ABX^{TM} (Apatech Ltd, UK) for spinal, orthopedic, periodontal, oral and craniomaxillofacial applications. SiHAs are intended to improve the bone formation compared to non-substituted HA, in terms of better bioactivity, higher osteoclastic resorption activity, enhanced bone

ingrowth, and bone implant coverage. This performance improvement could be due to the higher solubility at the grain boundary [9,10] and the osteogenic action of silicon in the early stages of bone formation [14]. SiHA approved for clinical use and most of HA based implants, undergo a sintering process at high temperatures to increase the density and improve the mechanical properties. This thermal treatment yields polycrystalline pieces or granulates constituted by large SiHA crystals, having dimensions of several micrometers depending on the crystal direction considered. Moreover, the crystalline growth comprises a reduction of porosity and surface area. In the last years, the possibility of enhancing the bioceramics bioreactivity through their preparation with low temperature methods has been suggested [15]. Avoiding the high temperature sintering process (commonly about 1200ºC), nanocrystalline pieces and grains can be prepared. The associated higher surface area and smaller crystal size could provide very interesting bioresponses, especially in SiHA as the osteogenic effect of silicon is mainly explained by its location at the crystals boundaries [9,10].

As essential processes after biomaterial-tissue contact, the albumin adsorption to both nanocrystalline HA and SiHA as well as the effects of these materials on different immune cells have been evaluated in the present study. With this objective, murine macrophages (main components of innate immune system) and T lymphocytes (specific cells involved in adaptive response) have been cultured for three days in direct contact with these nanocrystalline hydroxyapatites, as an *in vitro* model of the early immune response to both materials. Different cell parameters as morphology, proliferation, phagocytic activity, viability, lactate dehydrogenase release (LDH), apoptosis, intracellular reactive oxygen species (ROS), cell cycle phases, and cytokine (IL-6 and TNF-α) production were determined as markers of biocompatibility and specific response of both cell types.

2. Material and Methods

2.1. Nanocrystalline hydroxyapatite and silicon substituted hydroxyapatite synthesis

Samples of pure and silicon substituted HA were prepared by aqueous precipitation reaction of $Ca(NO_3)_2 \cdot 4H_2O$, $(NH_4)_2HPO_4$ and $Si(CH_3CH_2O)_4$ solutions. The amounts of reactants were calculated on the assumption that silicon would be substituted by phosphorus. Two different compositions have been prepared with nominal formula $Ca_{10}(PO_4)_{6-x}(SiO_4)_x(OH)_{2-x,}$ with x = 0 and 0.25 for nano-HA and nano-SiHA samples, respectively. 1M $Ca(NO_3)_2 \cdot 4H_2O$ solution was added to $(NH_4)_2HPO_4$ and TEOS solutions of stoichiometric concentration to obtain the compositions described above. The mixture was stirred for 12 hours at 80°C. During the reaction the pH was continuously adjusted to 9.5 to ensure constant conditions during the synthesis. The samples were treated at 700°C under air atmosphere to remove the nitrates without introducing important changes in the crystallite size respect to the as precipitated powder. The HA and Si-HA grains thus obtained have a diameter ranging in size between 10 to 100 micrometers, as determined by means of a Sedigraph 5100 equipment (data not shown).

2.2. Chemical, structural and microstructural studies of nano-HA and nano-SiHA

Elemental chemical analysis was carried out by fluorescence X-ray spectrometry for P, Si and Ca. XRD patterns were collected with a Philips PW 1730 X-ray diffractometer using Cu Kα radiation with a step size of 0.02 2θº and 8 seconds of counting time. In order to determine the crystalline and microstructural characteristic of both samples, Rietveld refinements were carried out over the XRD patterns collected. The refinements were performed using the atomic position set and the space group of the HA structure $P6_3/m$, no 176 [16] by means of computer program FullProf 2000.

2.3. Adsorption of bovine serum albumin (BSA)

Adsorption experiments were carried out with 10 mg of either nano-HA or nano-SiHA granulates incubated with different concentrations of BSA (Sigma) in PBS and moderately shaken for 5 h at 37ºC. Incubation of 24 h showed no significant difference in the amount of protein adsorbed. Controls with the same BSA concentration but without material were carried out. After incubation time, the supernatant obtained was analyzed by UV-Vis spectroscopy and the adsorbed protein amount was calculated as the difference in protein concentration before and after BSA adsorption, using a value of 0.667 as coefficient E (0.1%, 279 nm, 1 cm).

2.4. Isolation and culture of murine peritoneal macrophages

Normal macrophages were obtained from the peritoneum of untreated mice as described elsewhere [17]. Briefly, BALB/c mice were killed, and the skin was removed from the abdominal area. Mice were then injected intraperitoneally with 4-5 ml of phosphate buffered saline (PBS) using an 18 gauge needle. Without extracting the needle, the abdomen was gently massaged and then as much fluid from the peritoneum as possible was slowly withdrawn with the syringe. The peritoneal cells were washed in PBS before use. All procedures were approved by Institutional Animal Care and Use Committees.

2.5. Cell culture

RAW-264.7 cells or mouse peritoneal macrophages at a density of 10^5 cells/ml were seeded in 6 well culture plates in 2ml of Dulbecco's Modified Eagle Medium (DMEM) supplemented with 10% heat-inactivated fetal bovine serum (FBS) and 1mM L-glutamine. SR.D10 cells [18] derived from the murine $CD4^+$ Th2 cell line D10.G4.1 [19] were cultured in suspension in Click's medium supplemented with 10% FBS containing 5 U/ml mrIL-2, 10 U/ml mrIL-4, and 25 pg/ml mrIL-1 (IL medium) as previously described

[18,19]. After 3 days culture in the presence or the absence of 1mg/ml of either nano-HA or nano- SiHA, cells were collected in order to determine the number of cells. The attached RAW-264.7 cells were washed with PBS and harvested using cell scrapers. Murine peritoneal macrophages were washed with PBS and detached with PBS / 1mM EDTA at 4ºC. After these procedures, 10 µl of the suspensions of these cell types and 10 µl of SR.D10 lymphocytes were counted with a Neubauer hemocytometer in the presence of 0.2% Trypan Blue, which stains the dead cells, for the analysis of cell proliferation. Then, cell suspensions were centrifuged at 310xg for 10 min and resuspended in fresh medium for the analysis of different parameters by Flow Cytometry as described below (*2.8 section*).

2.6. Morphological studies by Confocal Microscopy

After fixation with 3.7% paraformaldehyde in PBS, samples were permeabilized with 0.1% Triton X-100, preincubated with PBS containing 1% BSA and incubated with rhodamine phalloidin to stain F-actin filaments. After cell nuclei staining with 3 µM DAPI, cells were examined by a LEICA SP2 Confocal Laser Scanning Microscope. The fluorescence of rhodamine was excited at 540 nm and measured at 565 nm. DAPI fluorescence was excited at 405 nm and measured at 420–480 nm. To observe the phagocytosis of Latex Beads-Rabbit IgG-FITC by macrophages, cells were incubated as described below (*2.8.3* section), fixed with paraformaldehyde and the FITC fluorescence was detected with filters for excitation and emission at 485 and 535 nm, respectively.

2.7. Lactate dehydrogenase (LDH) measurement

LDH was measured in the culture medium by an enzymatic method at 340 nm (Bio-Analítica) using a Beckman DU 640 UV-Visible spectrophotometer.

2.8. Flow Cytometry studies

After cell detachment (*2.5* section) and incubation with the different probes (as it is described below) the conditions for the data acquisition and analysis were established using negative and positive controls with the CellQuest Program of Becton Dickinson and these conditions were maintained during all the experiments. Each experiment was carried out three times and single representative experiments are displayed. For statistical significance, at least 10,000 cells were analyzed in each sample and the mean of the fluorescence emitted by these single cells was used.

2.8.1. Apoptosis detection

Cell suspensions were incubated with 5μg/ml Hoechst 33258 for 30 min in darkness. Hoechst fluorescence was excited at 350 nm and measured at 450 nm in a LSR Becton Dickinson Flow Cytometer. The percentage of cells in each cycle phase was calculated with the CellQuest Program of Becton Dickinson and the $SubG_1$ fraction was used as indicative of apoptosis.

2.8.2. Intracellular reactive oxygen species (ROS) content and cell viability

Cells were incubated for 30 min with 100 μM DCFH/DA. DCF fluorescence was excited by a 15 mW laser tuning to 488 nm and was measured with a 530/30 band pass filter in a FACScalibur Becton Dickinson Flow Cytometer. Cell viability was determined by propidium iodide (PI, 0.005%) exclusion test to stain the DNA of dead cells.

2.8.3. Phagocytosis assays

The phagocytosis of Latex Beads-Rabbit IgG-FITC by macrophages was evaluated by the Phagocytosis Assay Kit (IgG FITC) of Cayman Chemical Company. Cells were incubated overnight with 1μg/ml LPS (*E.coli* 055:B5) and Latex Beads-Rabbit IgG-FITC after treatment with the materials. FITC fluorescence was excited by a 15 mW laser tuning to 488 nm and measured with a 530/30 band pass filter in a FACScalibur Becton Dickinson Flow Cytometer.

2.9. Inflammatory cytokine detection

The amounts of TNF-α, and IL-6 in the culture medium were quantified by ELISA (Gen-Probe, Diaclone), carried out according to the manufacturer's instructions.

2.10. Measurement of Ca^{2+} levels in the culture medium

To know the effect of hydroxyapatite (HA) and silicon-doped hydroxyapatite (SiHA) on Ca^{2+} levels in the culture medium, Ca^{2+} was analyzed with an ILyte Electrolyte Analyzer.

2.11. Statistics

Data are expressed as means $\pm$ standard deviations of one representative experiment out of three experiments carried out in triplicate. Statistical analysis was performed using the Statistical Package for the Social Sciences (SPSS) version 19 software. Statistical comparisons were made by analysis of variance (ANOVA). Scheffé test was used for *post hoc* evaluations of differences among groups. $P < 0.05$ was considered as statistically significant.

3. Results and Discussion

3.1. Chemical, structural and microstructural properties of nano-HA and nano-SiHA

The Ca, P and Si contents of the HA and SiHA granules, determined by elemental chemical analysis (**Table I**), show that the experimental cationic composition is very similar to the theoretical one, indicating that the synthesis method applied allows the incorporation of the silicon into the precipitated powder of nano-SiHA. XRD patterns were collected for nano-HA and nano-SiHA samples, exhibiting almost identical profiles which are presented in **Figure 1**. All the diffraction maxima correspond to the reflections of an apatite phase. **Table II** shows the lattice parameters and the sizes of the crystallites calculated using the apparent sizes along the different directions, obtained from the microstructural parameters calculated from the Rietveld refinements. **Table II** shows the data along [*100*] and [*001*] directions as well as the

mean crystallite size. The crystallite sizes indicate an anisotropic growth along the c axis, [0 0 1] direction, resulting in crystallites with needle-like shapes similar to those found in the mineral component of bone [20]. Nano-HA crystallites are 48.2 nm and 27.6 nm in size for the longest and shortest dimensions, respectively. Besides, nano-SiHA crystallites are 32.9 nm and 19.1 nm for the same dimensions, thus indicating that the silicon incorporation seems to play a role on the crystalline growth decreasing the crystal size. Independently of the dimension considered, the crystallites of both samples are smaller than 50 nm, confirming that the grains of nano-HA and nano-SiHA are polycrystalline particles formed by numerous nanocrystallites.

3.2. Adsorption of bovine serum albumin (BSA) to nano-HA and nano-SiHA

Blood proteins are important factors in determining the *in vivo* acceptance of biomaterials [1]. The protein adsorption depends on the physico-chemical properties of the material [21] and is a key point in the initial cellular response to a biomaterial after implantation, affecting the cellular adhesion, differentiation and extracellular matrix production [1]. Since albumin is the most abundant serum protein, a comparative evaluation of the adsorption of different BSA concentrations on nano-HA and nano-SiHA surface was carried out. Both nanocrystalline hydroxyapatites showed similar BSA adsorption profiles (**Figure 2**), thus indicating that the incorporation of the silicon does not change the binding affinity and the maximum amount of protein adsorbed.

3.3. In vitro effects of nano-HA and nano-SiHA on immune cells

To know the nano-HA and nano-SiHA effects on immune system, macrophages and T lymphocytes were used as *in vitro* models of innate and adaptive immune response, respectively.

3.3.1. Macrophage response to nano-HA and nano-SiHA

The macrophage capability of playing both positive and negative roles in disease processes and tissue remodelling after injury, has been recently related to the diverse and context dependent macrophage phenotypes [6]. Thus, macrophages can be classified in two types: proinflammatory and microbicidal ones (M1) and immunomodulatory and reparative ones (M2) [22]. The host response to biomaterials depends on the balance between the M1 and M2 phenotypes, with participation of diverse specific cytokines. RAW-264.7 is a mouse macrophage cell line retaining many of the characteristics of macrophages *in vivo* [23]. **Figure 3** shows the results concerning proliferation and phagocytic activity of murine RAW-264.7 macrophages after 3 days of treatment with either nano-HA or nano-SiHA (1mg/ml). RAW-264.7 growth was significantly delayed by both hydroxyapatites in comparison with cells cultured in the absence of material (**Figure 3A**, $p<0.005$). Both materials also produced a significant decrease in phagocytic activity of RAW-264.7 cells ($p<0.005$), although these cells continued phagocyting when in contact with either nano-HA or nano-SiHA (**Figure 3B**). No significant alterations in cell viability and $SubG_1$ fraction reveal that neither nano-HA nor nano-SiHA induced apoptosis of RAW-264.7 cells (**Table III**). No significant changes of reactive oxygen species, widely used as macrophage signaling mediators [24], were observed after treatment with these materials, thus indicating the absence of oxidative stress in RAW-264.7 macrophages (**Table III**). The integrity of plasma membrane was demonstrated because no significant increase of LDH levels in the culture medium was detected (**Table III**). No morphological alterations induced by these nanocrystalline hydroxyapatites on these cells were observed (**Figure 4**). Studies with other cell types showed that silicon-doped hydroxyapatite has biocompatibility and mechanical properties comparable to HA but improved bioactivity which enhances bone tissue growth rate [11,25-27]. **Previous experiments carried out with human Saos-2 osteoblasts cultured for 4 days in the presence of 1 mg/ml of either nano-HA or nano-SiHA demonstrated that this cell type proliferated in contact with both materials, but the cell number was significantly lower**

than in controls. However, the number of Saos-2 cells in contact with nano-SiHA was significantly higher than with nano-HA, indicating that these cells grow better in the presence of nano-SiHA. This result was also observed by Scanning Electron Microscopy (SEM) when Saos-2 osteoblasts were cultured for 4 days on surface of both nano-HA and nano-SiHA disks. SEM images demonstrated that Saos-2 cells adhere to the nano-SiHA disks, proliferate and colonize their surface better than on HA disks. Although low levels of apoptosis were obtained in human Saos-2 osteoblasts after contact with these materials, this cell type showed a slight increase of cell apoptosis in the presence of nano-HA (2.1 %) in comparison to nano-SiHA (0.4%) and control cells (0.3%). Intracellular ROS content did not show alteration in the presence of these materials, thus indicating no oxidative stress [11].

To evaluate the effects of these nanocrystalline hydroxyapatites on a cellular model more similar to the *in vivo* situation, fresh murine macrophages were obtained from the peritoneum of untreated mice and were cultured for 3 days in the presence of either nano-HA or nano-SiHA (1mg/ml) to measure cell proliferation, phagocytic activity and release of inflammatory cytokines (IL-6, TNF-α). **Figure 5A** shows a significant proliferation decrease of fresh murine macrophages induced by both hydroxyapatites ($p<0.005$). Nano-SiHA material also produce a significant decrease in phagocytosis of these cells ($p<0.005$) whose activity is not affected by nano-HA (**Figure 5B**). In spite of this decrease induced by SiHA, fresh macrophages continue phagocyting when they are in contact with this material (**Figures 6A** and **6B)**. **The different effect of nano-HA on RAW and fresh macrophages can be due to the higher values of phagocytosis obtained with fresh macrophages which always showed higher fluorescence values (Figure 5 B) than RAW macrophages (Figure 3B). This fact can be associated with a lower sensitivity to nano-HA of fresh macrophages although the phagocytic activity of these cells was affected by nano-SiHA.**

Since the hydroxyapatite bioactivity could produce the sequestration of calcium in the extracellular medium, and taking into account that the Ca^{2+} ion plays a crucial role in cell processes [28], Ca^{2+} levels were measured in the culture medium. **Figure 7** shows a significant Ca^{2+} decrease in the culture medium produced by both nano-HA and nano-SiHA, more pronounced with nano-SiHA, in agreement with the higher bioactivity of this material [27]. The observed sequestration of extracellular calcium can be partially responsible of the lower proliferation produced by nano-HA and nano-SiHA, as it has been described in other cell types [29]. Concerning the possible effect of extracellular calcium depletion on phagocytosis, some studies have shown that macrophages can still phagocyte in the absence of calcium through Fc receptor mediated pathways [30]. On the other hand, the changes due to depletion of extracellular calcium could be decreased *in vivo* by the dynamic flow conditions of the body fluids [31].

It is well known that interleukin 6 (IL-6) and tumor necrosis factor alpha (TNF- α) are major inflammatory cytokines and play a crucial role in infection, inflammation and stress responses. For this reason, the release of IL-6 and TNF- α by fresh mouse macrophages was measured after 3 days of treatment with these materials. **Figure 8A** shows significant increases of IL-6 induced by nano-HA ($p<0.05$) and nano-SiHA ($p<0.005$). Both materials also triggered a significant TNF-α increase (**Figure 8B**), which was more pronounced with nano-HA ($p<0.005$) than with nano-SiHA ($p<0.05$). These results evidence the early *in vitro* response of macrophages to both nanocrystalline hydroxyapatites, suggesting that, after *in vivo* implantation, these biomaterials might induce activation of the innate immune system and production of pro-inflammatory cytokines. Although further studies are needed to elucidate the long-term response of macrophages to these materials, an *in vivo* study evidenced the moderate IL-6 and IL-8 expression in bone cells and rich IL10–containing cells distribution after 8 months of hydroxyapatite implantation [32]. This fact reveals the switch of

pro-inflammatory macrophage phenotype (M1) to reparative phenotype (M2) expressing high levels of IL-10 [6] and indicates the resolution of inflammatory phase at longer times.

3.3.2. Lymphocyte response to nano-HA and nano-SiHA

T lymphocytes also play an important regulatory role in the resolution of the inflammatory process through local secretion of cytokines and chemokines, many of which are known to affect macrophage polarization [6]. In order to know the nano-HA and nano-SiHA effects on T lymphocytes as specific cells involved in adaptive immune response, SR.D10 cells were cultured in the presence of these materials (1mg/ml). SR.D10 [18] is a clone obtained from the murine $CD4^+$ Th2 cell line D10.G4.1 [19] specific for Conalbumin fragment 134–146, bound to $I\text{-}A^k$ class II major histocompatibility complex molecules. SR.D10 cells provide a convenient system to test in vitro lymphocyte activation which has been largely used as a model of T cell proliferation and signalling [33,34]. These T cells have been previously used for biocompatibility testing of different bioceramics [4]. Although non-significant differences were observed on proliferation and viability of SR.D10 lymphocytes after 3 days treatment (**Figures 9A** and **9B**), a significant increase of Sub G_1 fraction, indicative of cell apoptosis, is produced by both hydroxyapatites. This effect is accompanied by significant decreases of both S and G2M fractions (**Figure 10**).

Programmed cell death (apoptosis) is a key mechanism for regulating lymphocyte number. In T lymphocytes, two major mechanisms have been described involving: a) the activation of T cell through Fas, which leads to the caspase-8 and caspase-3 induction, and b) the loss of mitochondrial integrity controlled by members of the BcL-2 family proteins [35]. Other molecules that regulate this death process include the leukocyte common antigen CD45, which has been shown to be essential for normal signaling through the T cell receptor (TCR) and for modulating signaling through cytokine receptors [50]. SR.D10 "syngeneic-reactive D10", is a variant of the murine $CD4^+$ T helper cell clone which is hyperreactive to TCR dependent and-independent stimuli. This hyperreactivity is related to the expression of several

cell surface molecules involved in T cell activation as CD45 RB receptor, abundantly expressed in SR.D10 [18]. The high levels of T cell apoptosis observed in the present study could be explained by the abundant expression of this receptor that favors this death process through Fas and TCR-induced apoptosis [36]. The presence of either nano-HA or nano-SiHA produces a significant increase of SR.D10 apoptosis probably through these mechanisms.

All these studies and previous results obtained with many different biomaterials demonstrate different cellular responses which are dependent on each biomaterial and depending on each cell type [37-39].

4. Conclusions

The *in vitro* evaluation of the early immune response to nanocrystalline hydroxyapatites evidences significant decreases of macrophage proliferation and phagocytic activity. These biomaterials also induce the production of the pro-inflammatory cytokines IL-6 and TNF-α by murine fresh macrophages and trigger apoptosis mechanisms in SR.D10 T lymphocytes. The study of the early immune response is the first step to know whether a phenotypic switch of pro-inflammatory (M1) to reparative macrophages (M2) occurs in the presence of these materials. The results obtained will be used in further studies to elucidate the long-term response of immune cells to these nanocrystalline hydroxyapatites which conditions the biomaterial success or rejection. The detection of specific macrophage markers and cytokines will allow a better understanding of the effects at longer times of these biomaterials on the equilibrium of these two distinct macrophage subsets which represents a key factor for establishing their applicability for bone Tissue Engineering.

Acknowledgements

This study was supported by research grants from Comunidad de Madrid through the project S2009/MAT-1472 and the Ministerio de Ciencia e Innovacion (MICINN) through the projects MAT2012-35556 and CSO2010-11384-E (Agening Network of Excellence). J.M. Rojo is supported by Grant PI10/00650 from "Plan Estatal I+D+i, ISCIII-Subdirección General de Evaluación y Fomento de la Investigación, Ministerio de Economía y Competitividad (MINECO), Spain. M.C. Matesanz is greatly indebted to MICINN for the predoctoral fellowship. The authors wish to thank also to Javier Linares for technical assistance and to the staff of the Cytometry and Fluorescence Microscopy Center of the Universidad Complutense de Madrid (Spain).

References

1. Wilson CJ, Clegg RE, Leavesley DI, Pearcy MJ. Mediation of biomaterial-cell interactions by adsorbed proteins: a review. Tissue Eng 2005;11:1-18.
2. Gorbet MB, Sefton MV. Biomaterial-associated thrombosis: roles of coagulation factors, complement, platelets and leukocytes. Biomaterials 2004;25:5681-5703.
3. Smith MJ, White KL Jr, Smith DC, Bowlin GL. *In vitro* evaluations of innate and acquired immune responses to electrospun polydioxanone-elastin blends. Biomaterials 2009;30:149-159.
4. Alcaide M, Portolés P, López-Noriega A, Arcos D, Vallet-Regí M, Portolés MT. Interaction of an ordered mesoporous bioactive glass with osteoblasts, fibroblasts and lymphocytes, demonstrating its biocompatibility as a potential bone graft material. Acta Biomaterialia 2010;6:892-899.
5. Medzhitov R, Janeway CA Jr. Innate immunity. N Engl J Med 2000;343:338-344.
6. Brown BN, Ratner BD, Goodman SB, Amar S, Badylak SF. Macrophage polarization: an opportunity for improved outcomes in biomaterials and regenerative medicine. Biomaterials 2012;33:3792-3802.

7. Franz S, Rammelt S, Scharnweber D, Simon JC. Immune responses to implants: a review of the implications for the design of immunomodulatory biomaterials. Biomaterials 2011;32:6692-6709.
8. Dorozhkin SV. Bioceramics of calcium orthophosphates. Biomaterials 2010;31:1465-1485.
9. Vallet-Regí M, Arcos D. Silicon substituted hydroxyapatites. A method to upgrade calcium phosphate based implants. J Mater Chem 2005;15:1509-1516.
10. Porter AE, Patel N, Skepper JN, Best SM, Bonfield W. Comparison of *in vivo* dissolution processes in hydroxyapatite and silicon-substituted hydroxyapatite bioceramics. Biomaterials 2003;24:4609-4620.
11. Matesanz MC, Feito MJ, Ramírez-Santillán C, Lozano RM, Sánchez-Salcedo S, Arcos D, Vallet-Regí M, Portolés MT. Signaling pathways of immobilized FGF-2 on silicon-substituted hydroxyapatite. Macromol Biosci 2012;12:446-453.
12. Balamurugan A, Rebelo AHS, Lemos AF, Rocha JHG, Ventura JMG, Ferreira JMF. Suitability evaluation of sol-gel derived Si-substituted hydroxyapatite for dental and maxillofacial applications through *in vitro* osteoblasts response. Dent Mater 2008;24:1374-1380.
13. Arcos D, Rodríguez-Carvajal J, Vallet-Regí M. Silicon incorporation in hydroxyapatite obtained by controlled crystallization. Chem Mater 2004;16:2300-2308.
14. Carlisle EM. Silicon: a requirement in bone formation independent of vitamin D_1. Calcif Tissue Int 1981;33:27-34.
15. Dorozhkin SV. Nanodimensional and nanocrystalline apatites and other calcium orthophosphates in biomedical engineering, biology and medicine. Materials 2009;2:1975-2045.

16. Kay MI, Young RA, Posner AS. Crystal structure of hydroxyapatite. Nature 1964;204:1050-1052.

17. Mishell BB, Shiigi JM. Preparation of mouse cell suspensions. In: Mishell BB, Shiigi JM, editors. Selected Methods in Cellular Immunology. San Francisco: WH Freeman & Co., 1980. p.1-28.

18. Ojeda G, Ronda M, Ballester S, Díez-Orejas R, Feito MJ, García-Albert L, Rojo JM, Portolés P. A hyperreactive variant of a $CD4^+$ T cell line is activated by syngeneic antigen presenting cells in the absence of antigen. Cell Immunol 1995;164:265-278.

19. Kaye J, Porcelli S, Tite J, Jones B, Janeway CA Jr. Both a monoclonal antibody and antisera specific for determinants unique to individual cloned helper T cell lines can substitute for antigen and antigen-presenting cells in the activation of T cells. J Exp Med 1983;158:836-856.

20. Robinson RA. An electron-microscopic study of the crystalline inorganic component of bone and its relationship to the organic matrix. J Bone Joint Surg Am, 1952; 34:389-476.

21. Rosengren A, Pavlovic E, Oscarsson S, Krajewski A, Ravaglioli A, Piancastelli A. Plasma protein adsorption pattern on characterized ceramic biomaterials. Biomaterials 2002;23:1237–1247.

22. Kou PM, Babensee JE. Macrophage and dendritic cell phenotypic diversity in the context of biomaterials. J Biomed Mat Res A 2011;96:239-260.

23. Scheel J, Weimans S, Thiemann A, Heisler E, Hermann M. Exposure of the murine RAW-264.7 macrophage cell line to hydroxyapatite dispersions of various composition and morphology: assessment of cytotoxicity, activation and stress response. Toxicol in Vitro 2009;23:531-538.

24. Nagata M. Inflammatory cells and oxygen radicals. Curr Drug Targets Inflamm Allergy 2005;4:503-504.

25. Vallet-Regí M, Ruiz-Hernández E. Bioceramics: from bone regeneration to cancer nanomedicine. Adv Mater 2011;23:5177-5218.

26. Thian ES, Huang J, Best SM, Barber ZH, Brooks RA, Rushton N, Bonfield W. The response of osteoblasts to nanocrystalline silicon-substituted hydroxyapatite thin films. Biomaterials 2006;27:2692-2698.

27. Pietak AM, Reid JW, Stott MJ, Sayer M. Silicon substitution in the calcium phosphate bioceramics. Biomaterials 2007;28:4023-4032.

28. Zhivotovskya B, Orreniusa S. Calcium and cell death mechanisms: a perspective from the cell death community. Cell Calcium 2011;50:211-221.

29. Dvorak MM, Siddiqua A, Ward DT, Carter DH, Dallas SL, Nemeth EF, Riccardi D. Physiological changes in extracellular calcium concentration directly control osteoblast function in the absence of calciotropic hormones. Proc Nat Acad Sci USA 2004;101:5140-5145.

30. Jesse TM, Swanson JA. Calcium spikes in activated macrophages during Fcγ receptor-mediated phagocytosis. J Leukoc Biol 2002;72: 677-684.

31. da Silva HM, Mateescu M, Damia C, Champion E, Soares G, Anselme K. Importance of dynamic culture for evaluating osteoblast activity on dense silicon substituted hydroxyapatite. Colloids Surf B: Biointerfaces 2010;80:138-144.

32. Pilmane M, Salms G, Skagers A. Characterization of molecular events in the jaw of experimental animals after different time of hydroxyapatite (HAP) implantation. Int J Oral Maxillofac Surg 2001;40:1211-1218.

33. Díez-Orejas R, Ballester S, Feito MJ, Ojeda G, Criado G, Ronda M, Portolés P, Rojo JM. Genetic and immunochemical evidence for CD4-dependent association of $p56^{lck}$ with the αβ T-cell receptor (TCR): regulation of TCR-induced activation. EMBO J 1994;13:90-99.

34. Rojo JM, Janeway CA Jr. The biologic activity of anti-T cell receptor V region monoclonal antibodies is determined by the epitope recognized. J Immunol 1988;140:1081-1088.

35. Liu Z, Dawes R, Petrova S, Beverley PCL, Tchilian EZ . CD45 regulates apoptosis in peripheral T lymphocytes. Int Immunol 2005;18:959–966.

36. Ramaswamy M, Cruz AC, Cleland SY, Deng M, Price S, Rao VK, Siegel RM. Specific elimination of effector memory $CD4^+$ T cells due to enhanced Fas signaling complex formation and association with lipid raft microdomains. Cell Death Differ 2011;18:712-720.

37. Serrano MC, Pagani R, Vallet-Regí M, Peña J, Rámila A, Izquierdo I, Portolés MT. In vitro biocompatibility assessment of poly(ε-caprolactone) films using L929 mouse fibroblast. Biomaterials 2004;25:5603-5611.

38. Alcaide M, Portolés P, López-Noriega A, Arcos D, Vallet-Regí M, Portolés MT. Interaction of an ordered mesoporous bioactive glass with osteoblasts, fibroblasts and lymphocytes demonstrates its biocompatibility as a potential bone graft material. Acta Biomater 2010;6:892-899.

39. Cicuéndez M, Portolés MT, Izquierdo-Barba I, Vallet-Regí M. New nanocomposite system with nanocrystalline apatite embedded into mesoporous bioactive glass. Chem Mater 2012;24:1100-1106.

Figure Legends

Figure 1. Experimental (circles) and calculated (solid line) powder X-ray diffraction pattern for (up) nano-HA and (down) nano-SiHA.

Figure 2. BSA adsorption profiles on nano-HA and nano-SiHA after 5 hours treatment.

Figure 3. Effects of nano-HA and nano-SiHA on proliferation (A) and phagocytosis (B) of murine RAW-264.7 macrophages after 3 days treatment. ***$p<0.005$.

Figure 4. Morphology evaluation by confocal microscopy of murine RAW-264.7 macrophages after 3 days treatment with nano-HA (B) and nano-SiHA (C). Controls without material are also included (A). Detail of RAW-264.7 cells in the presence of nano-SiHA (D).

Figure 5. Effects of nano-HA and nano-SiHA on proliferation (A) and phagocytosis (B) of murine fresh macrophages after 3 days treatment. ***$p<0.005$.

Figure 6. Morphology evaluation by confocal microscopy of phagocytosis of rabbit IgG-FITC-coated latex beads (in green) by murine fresh macrophages after 3 days treatment with nano-SiHA. A) Panoramic image. B) Detail of the macrophage phagocyting activity.

Figure 7. Effects of nano-HA and nano-SiHA on Ca^{2+} levels in the culture medium after 3 days treatment. *$p<0.05$.

Figure 8. Effects of nano-HA and nano-SiHA on IL-6 (A) and TNF-α (B) release by murine fresh macrophages after 3 days treatment. *$p<0.05$, ***$p<0.005$.

Figure 9. Effects of nano-HA and nano-SiHA on proliferation (A) and viability (B) of SR.D10 lymphocytes after 3 days treatment.

Figure 10. Effects of nano-HA and nano-SiHA on cell cycle phases of SR.D10 lymphocytes after 3 days treatment. *$p<0.05$, ***$p<0.005$.

Table I. Experimental Ca, P and Si content (% in weight) obtained by X-ray fluorescence spectroscopy. Theoretical values are indicated below in brackets.

Table II. Lattice parameters and crystallite sizes obtained from Rietveld refinements. [(a)] The values in brackets for mean crystallite size do not make reference to the measurement errors, but are an estimation of the crystal size anisotropy.

Table III. Effects of nano-HA and nano-SiHA on cell viability, apoptosis, ROS production and LDH release into the culture medium of murine RAW-264.7 macrophages after 3 days treatment.

EARLY *IN VITRO* RESPONSE OF MACROPHAGES AND T LYMPHOCYTES TO NANOCRYSTALLINE HYDROXYAPATITES

María Concepción Matesanz[a], María José Feito[a], Mercedes Oñaderra[a], Cecilia Ramírez-Santillán[a], Carmen da Casa[a], Daniel Arcos[b,c], María Vallet-Regí[b,c], José María Rojo[d], María Teresa Portolés [a*]

[a]Department of Biochemistry and Molecular Biology I, Faculty of Chemistry, Universidad Complutense, 28040-Madrid, Spain

conchitamatesanz@hotmail.com, mjfeito@pdi.ucm.es, monaderr@bio.ucm.es, cecilia27884@hotmail.com, cdacasa_19991@hotmail.com, portoles@quim.ucm.es

[b]Department of Inorganic and Bioinorganic Chemistry, Faculty of Pharmacy, UCM, Instituto de Investigación Sanitaria Hospital 12 de Octubre i+12, 28040-Madrid, Spain

arcosd@farm.ucm.es, vallet@farm.ucm.es

[c]Networking Research Center on Bioengineering, Biomaterials and Nanomedicine, CIBER-BBN, Spain

[d]Department of Cellular and Molecular Medicine, Centro de Investigaciones Biológicas, CSIC, 28040-Madrid, Spain

jmrojo@cib.csic.es

* Corresponding author: Prof. María Teresa Portolés. Departamento de Bioquímica y Biología Molecular I, Facultad de Ciencias Químicas, Universidad Complutense, 28040-Madrid, Spain. Telephone: 34-1-394 46 66, Fax: 34-1-394 41 59, E-mail: portoles@quim.ucm.es

Abstract

Hypothesis

Synthetic hydroxyapatite (HA) and Si substituted hydroxyapatite (SiHA) are calcium phosphate ceramics currently used in the field of dentistry and orthopaedic surgery. The preparation of both biomaterials as polycrystalline solid pieces or grains formed by nanocrystallites has awakened a great interest to enhance the bioactive behavior due to the microstructural defects and the higher surface area. The study of the macrophage and lymphocyte behavior in contact with nanocrystalline HA and SiHA will allow to elucidate the immune response which conditions the success or rejection of these biomaterials.

Experiments

HA and SiHA granules (with sizes of tens of microns) have been prepared by controlled aqueous precipitation avoiding subsequent high temperature sintering. HA and SiHA granules were constituted by crystallites smaller than 50 nm. The effects of both nanocrystalline materials on immune system have been evaluated with macrophages (main components of innate immune system) and T lymphocytes (specific cells of adaptive response) after short-term culture as *in vitro* models of the early immune response.

Findings

Significant decreases of macrophage proliferation and phagocytic activity, increased production of inflammatory cytokines (IL-6, TNF-α) and T lymphocyte apoptosis, were induced by these nanocrystalline ceramics suggesting that, after *in vivo* implantation, they induce significant effects on immune responses, including an early activation of the innate immune system.

Keywords: biocompatibility, cytokine, hydroxyapatite, lymphocyte, macrophage.

1. Introduction

Immediately after biomaterial-tissue contact, blood and interstitial fluid proteins adsorb to the biomaterial surface and activate the coagulation cascade, complement system, platelets and immune cells [1,2]. Thus, the evaluation of serum proteins adsorption and the biomaterial effects on immune system are essential aspects of biocompatibility assessment [3,4]. The immune response comprises both innate and adaptive defence mechanisms which co-ordinately activate different cell populations. Neutrophils, monocytes and macrophages are critical cellular components of the innate immune response, carrying out phagocytosis and producing reactive oxygen species, antimicrobial peptides, and inflammatory mediators [5]. The adaptive response is mediated by antigen-specific lymphocytes (T and B cells) and by their products, which include inflammatory cytokines and antibodies. Although the interaction of immune cells with biomaterials has been considered negative for a long time, specific cell responses may be beneficial for biomaterial integration and improve implant performance [6]. Recent studies demonstrate the potential of biomaterials to modulate immune cell function suggesting the possibility of designing biomaterials capable of eliciting appropriate immune responses at implantation sites [7].

Because of its similarity to the mineral component of bone, synthetic hydroxyapatite (HA) is a calcium phosphate ceramic widely used in the field of dentistry and orthopaedic surgery with different purposes. Its main applications are grafting for small bone defects, coatings of metallic prostheses and periodontal implants, and as scaffolds for bone tissue engineering [8]. Silicon substituted hydroxyapatites (SiHAs) have attracted the attention of many researchers [9-13] and have recently been incorporated to the biomaterials market as Actifuse ABX^{TM} (Apatech Ltd, UK) for spinal, orthopedic, periodontal, oral and craniomaxillofacial applications. SiHAs are intended to improve the bone formation compared to non-substituted HA, in terms of better bioactivity, higher osteoclastic resorption activity, enhanced bone

ingrowth, and bone implant coverage. This performance improvement could be due to the higher solubility at the grain boundary [9,10] and the osteogenic action of silicon in the early stages of bone formation [14]. SiHA approved for clinical use and most of HA based implants, undergo a sintering process at high temperatures to increase the density and improve the mechanical properties. This thermal treatment yields polycrystalline pieces or granulates constituted by large SiHA crystals, having dimensions of several micrometers depending on the crystal direction considered. Moreover, the crystalline growth comprises a reduction of porosity and surface area. In the last years, the possibility of enhancing the bioceramics bioreactivity through their preparation with low temperature methods has been suggested [15]. Avoiding the high temperature sintering process (commonly about 1200ºC), nanocrystalline pieces and grains can be prepared. The associated higher surface area and smaller crystal size could provide very interesting bioresponses, especially in SiHA as the osteogenic effect of silicon is mainly explained by its location at the crystals boundaries [9,10].

As essential processes after biomaterial-tissue contact, the albumin adsorption to both nanocrystalline HA and SiHA as well as the effects of these materials on different immune cells have been evaluated in the present study. With this objective, murine macrophages (main components of innate immune system) and T lymphocytes (specific cells involved in adaptive response) have been cultured for three days in direct contact with these nanocrystalline hydroxyapatites, as an *in vitro* model of the early immune response to both materials. Different cell parameters as morphology, proliferation, phagocytic activity, viability, lactate dehydrogenase release (LDH), apoptosis, intracellular reactive oxygen species (ROS), cell cycle phases, and cytokine (IL-6 and TNF-α) production were determined as markers of biocompatibility and specific response of both cell types.

2. Material and Methods

2.1. Nanocrystalline hydroxyapatite and silicon substituted hydroxyapatite synthesis

Samples of pure and silicon substituted HA were prepared by aqueous precipitation reaction of $Ca(NO_3)_2 \cdot 4H_2O$, $(NH_4)_2HPO_4$ and $Si(CH_3CH_2O)_4$ solutions. The amounts of reactants were calculated on the assumption that silicon would be substituted by phosphorus. Two different compositions have been prepared with nominal formula $Ca_{10}(PO_4)_{6-x}(SiO_4)_x(OH)_{2-x,}$ with x = 0 and 0.25 for nano-HA and nano-SiHA samples, respectively. 1M $Ca(NO_3)_2 \cdot 4H_2O$ solution was added to $(NH_4)_2HPO_4$ and TEOS solutions of stoichiometric concentration to obtain the compositions described above. The mixture was stirred for 12 hours at 80°C. During the reaction the pH was continuously adjusted to 9.5 to ensure constant conditions during the synthesis. The samples were treated at 700°C under air atmosphere to remove the nitrates without introducing important changes in the crystallite size respect to the as precipitated powder. The HA and Si-HA grains thus obtained have a diameter ranging in size between 10 to 100 micrometers, as determined by means of a Sedigraph 5100 equipment (data not shown).

2.2. Chemical, structural and microstructural studies of nano-HA and nano-SiHA

Elemental chemical analysis was carried out by fluorescence X-ray spectrometry for P, Si and Ca. XRD patterns were collected with a Philips PW 1730 X-ray diffractometer using Cu Kα radiation with a step size of 0.02 2θº and 8 seconds of counting time. In order to determine the crystalline and microstructural characteristic of both samples, Rietveld refinements were carried out over the XRD patterns collected. The refinements were performed using the atomic position set and the space group of the HA structure $P6_3/m$, no 176 [16] by means of computer program FullProf 2000.

2.3. Adsorption of bovine serum albumin (BSA)

Adsorption experiments were carried out with 10 mg of either nano-HA or nano-SiHA granulates incubated with different concentrations of BSA (Sigma) in PBS and moderately shaken for 5 h at 37ºC. Incubation of 24 h showed no significant difference in the amount of protein adsorbed. Controls with the same BSA concentration but without material were carried out. After incubation time, the supernatant obtained was analyzed by UV-Vis spectroscopy and the adsorbed protein amount was calculated as the difference in protein concentration before and after BSA adsorption, using a value of 0.667 as coefficient E (0.1%, 279 nm, 1 cm).

2.4. Isolation and culture of murine peritoneal macrophages

Normal macrophages were obtained from the peritoneum of untreated mice as described elsewhere [17]. Briefly, BALB/c mice were killed, and the skin was removed from the abdominal area. Mice were then injected intraperitoneally with 4-5 ml of phosphate buffered saline (PBS) using an 18 gauge needle. Without extracting the needle, the abdomen was gently massaged and then as much fluid from the peritoneum as possible was slowly withdrawn with the syringe. The peritoneal cells were washed in PBS before use. All procedures were approved by Institutional Animal Care and Use Committees.

2.5. Cell culture

RAW-264.7 cells or mouse peritoneal macrophages at a density of 10^5 cells/ml were seeded in 6 well culture plates in 2ml of Dulbecco's Modified Eagle Medium (DMEM) supplemented with 10% heat-inactivated fetal bovine serum (FBS) and 1mM L-glutamine. SR.D10 cells [18] derived from the murine $CD4^+$ Th2 cell line D10.G4.1 [19] were cultured in suspension in Click's medium supplemented with 10% FBS containing 5 U/ml mrIL-2, 10 U/ml mrIL-4, and 25 pg/ml mrIL-1 (IL medium) as previously described

[18,19]. After 3 days culture in the presence or the absence of 1mg/ml of either nano-HA or nano- SiHA, cells were collected in order to determine the number of cells. The attached RAW-264.7 cells were washed with PBS and harvested using cell scrapers. Murine peritoneal macrophages were washed with PBS and detached with PBS / 1mM EDTA at 4ºC. After these procedures, 10 µl of the suspensions of these cell types and 10 µl of SR.D10 lymphocytes were counted with a Neubauer hemocytometer in the presence of 0.2% Trypan Blue, which stains the dead cells, for the analysis of cell proliferation. Then, cell suspensions were centrifuged at 310xg for 10 min and resuspended in fresh medium for the analysis of different parameters by Flow Cytometry as described below (*2.8 section*).

2.6. Morphological studies by Confocal Microscopy

After fixation with 3.7% paraformaldehyde in PBS, samples were permeabilized with 0.1% Triton X-100, preincubated with PBS containing 1% BSA and incubated with rhodamine phalloidin to stain F-actin filaments. After cell nuclei staining with 3 µM DAPI, cells were examined by a LEICA SP2 Confocal Laser Scanning Microscope. The fluorescence of rhodamine was excited at 540 nm and measured at 565 nm. DAPI fluorescence was excited at 405 nm and measured at 420–480 nm. To observe the phagocytosis of Latex Beads-Rabbit IgG-FITC by macrophages, cells were incubated as described below (*2.8.3* section), fixed with paraformaldehyde and the FITC fluorescence was detected with filters for excitation and emission at 485 and 535 nm, respectively.

2.7. Lactate dehydrogenase (LDH) measurement

LDH was measured in the culture medium by an enzymatic method at 340 nm (Bio-Analítica) using a Beckman DU 640 UV-Visible spectrophotometer.

2.8. Flow Cytometry studies

After cell detachment (*2.5* section) and incubation with the different probes (as it is described below) the conditions for the data acquisition and analysis were established using negative and positive controls with the CellQuest Program of Becton Dickinson and these conditions were maintained during all the experiments. Each experiment was carried out three times and single representative experiments are displayed. For statistical significance, at least 10,000 cells were analyzed in each sample and the mean of the fluorescence emitted by these single cells was used.

2.8.1. Apoptosis detection

Cell suspensions were incubated with 5μg/ml Hoechst 33258 for 30 min in darkness. Hoechst fluorescence was excited at 350 nm and measured at 450 nm in a LSR Becton Dickinson Flow Cytometer. The percentage of cells in each cycle phase was calculated with the CellQuest Program of Becton Dickinson and the $SubG_1$ fraction was used as indicative of apoptosis.

2.8.2. Intracellular reactive oxygen species (ROS) content and cell viability

Cells were incubated for 30 min with 100 μM DCFH/DA. DCF fluorescence was excited by a 15 mW laser tuning to 488 nm and was measured with a 530/30 band pass filter in a FACScalibur Becton Dickinson Flow Cytometer. Cell viability was determined by propidium iodide (PI, 0.005%) exclusion test to stain the DNA of dead cells.

2.8.3. Phagocytosis assays

The phagocytosis of Latex Beads-Rabbit IgG-FITC by macrophages was evaluated by the Phagocytosis Assay Kit (IgG FITC) of Cayman Chemical Company. Cells were incubated overnight with 1μg/ml LPS (*E.coli* 055:B5) and Latex Beads-Rabbit IgG-FITC after treatment with the materials. FITC fluorescence was excited by a 15 mW laser tuning to 488 nm and measured with a 530/30 band pass filter in a FACScalibur Becton Dickinson Flow Cytometer.

2.9. Inflammatory cytokine detection

The amounts of TNF-α, and IL-6 in the culture medium were quantified by ELISA (Gen-Probe, Diaclone), carried out according to the manufacturer's instructions.

2.10. Measurement of Ca^{2+} levels in the culture medium

To know the effect of hydroxyapatite (HA) and silicon-doped hydroxyapatite (SiHA) on Ca^{2+} levels in the culture medium, Ca^{2+} was analyzed with an ILyte Electrolyte Analyzer.

2.11. Statistics

Data are expressed as means $\pm$ standard deviations of one representative experiment out of three experiments carried out in triplicate. Statistical analysis was performed using the Statistical Package for the Social Sciences (SPSS) version 19 software. Statistical comparisons were made by analysis of variance (ANOVA). Scheffé test was used for *post hoc* evaluations of differences among groups. $P < 0.05$ was considered as statistically significant.

3. Results and Discussion

3.1. Chemical, structural and microstructural properties of nano-HA and nano-SiHA

The Ca, P and Si contents of the HA and SiHA granules, determined by elemental chemical analysis (**Table I**), show that the experimental cationic composition is very similar to the theoretical one, indicating that the synthesis method applied allows the incorporation of the silicon into the precipitated powder of nano-SiHA. XRD patterns were collected for nano-HA and nano-SiHA samples, exhibiting almost identical profiles which are presented in **Figure 1**. All the diffraction maxima correspond to the reflections of an apatite phase. **Table II** shows the lattice parameters and the sizes of the crystallites calculated using the apparent sizes along the different directions, obtained from the microstructural parameters calculated from the Rietveld refinements. **Table II** shows the data along [*100*] and [*001*] directions as well as the

mean crystallite size. The crystallite sizes indicate an anisotropic growth along the c axis, [0 0 1] direction, resulting in crystallites with needle-like shapes similar to those found in the mineral component of bone [20]. Nano-HA crystallites are 48.2 nm and 27.6 nm in size for the longest and shortest dimensions, respectively. Besides, nano-SiHA crystallites are 32.9 nm and 19.1 nm for the same dimensions, thus indicating that the silicon incorporation seems to play a role on the crystalline growth decreasing the crystal size. Independently of the dimension considered, the crystallites of both samples are smaller than 50 nm, confirming that the grains of nano-HA and nano-SiHA are polycrystalline particles formed by numerous nanocrystallites.

3.2. Adsorption of bovine serum albumin (BSA) to nano-HA and nano-SiHA

Blood proteins are important factors in determining the *in vivo* acceptance of biomaterials [1]. The protein adsorption depends on the physico-chemical properties of the material [21] and is a key point in the initial cellular response to a biomaterial after implantation, affecting the cellular adhesion, differentiation and extracellular matrix production [1]. Since albumin is the most abundant serum protein, a comparative evaluation of the adsorption of different BSA concentrations on nano-HA and nano-SiHA surface was carried out. Both nanocrystalline hydroxyapatites showed similar BSA adsorption profiles (**Figure 2**), thus indicating that the incorporation of the silicon does not change the binding affinity and the maximum amount of protein adsorbed.

3.3. In vitro effects of nano-HA and nano-SiHA on immune cells

To know the nano-HA and nano-SiHA effects on immune system, macrophages and T lymphocytes were used as *in vitro* models of innate and adaptive immune response, respectively.

3.3.1. Macrophage response to nano-HA and nano-SiHA

The macrophage capability of playing both positive and negative roles in disease processes and tissue remodelling after injury, has been recently related to the diverse and context dependent macrophage phenotypes [6]. Thus, macrophages can be classified in two types: proinflammatory and microbicidal ones (M1) and immunomodulatory and reparative ones (M2) [22]. The host response to biomaterials depends on the balance between the M1 and M2 phenotypes, with participation of diverse specific cytokines. RAW-264.7 is a mouse macrophage cell line retaining many of the characteristics of macrophages *in vivo* [23]. **Figure 3** shows the results concerning proliferation and phagocytic activity of murine RAW-264.7 macrophages after 3 days of treatment with either nano-HA or nano-SiHA (1mg/ml). RAW-264.7 growth was significantly delayed by both hydroxyapatites in comparison with cells cultured in the absence of material (**Figure 3A**, $p<0.005$). Both materials also produced a significant decrease in phagocytic activity of RAW-264.7 cells ($p<0.005$), although these cells continued phagocyting when in contact with either nano-HA or nano-SiHA (**Figure 3B**). No significant alterations in cell viability and $SubG_1$ fraction reveal that neither nano-HA nor nano-SiHA induced apoptosis of RAW-264.7 cells (**Table III**). No significant changes of reactive oxygen species, widely used as macrophage signaling mediators [24], were observed after treatment with these materials, thus indicating the absence of oxidative stress in RAW-264.7 macrophages (**Table III**). The integrity of plasma membrane was demonstrated because no significant increase of LDH levels in the culture medium was detected (**Table III**). No morphological alterations induced by these nanocrystalline hydroxyapatites on these cells were observed (**Figure 4**). Studies with other cell types showed that silicon-doped hydroxyapatite has biocompatibility and mechanical properties comparable to HA but improved bioactivity which enhances bone tissue growth rate [11,25-27]. Previous experiments carried out with human Saos-2 osteoblasts cultured for 4 days in the presence of 1 mg/ml of either nano-HA or nano-SiHA demonstrated that this cell type proliferated in contact with both materials, but the cell number was significantly lower than in controls.

However, the number of Saos-2 cells in contact with nano-SiHA was significantly higher than with nano-HA, indicating that these cells grow better in the presence of nano-SiHA. This result was also observed by Scanning Electron Microscopy (SEM) when Saos-2 osteoblasts were cultured for 4 days on surface of both nano-HA and nano-SiHA disks. SEM images demonstrated that Saos-2 cells adhere to the nano-SiHA disks, proliferate and colonize their surface better than on HA disks. Although low levels of apoptosis were obtained in human Saos-2 osteoblasts after contact with these materials, this cell type showed a slight increase of cell apoptosis in the presence of nano-HA (2.1 %) in comparison to nano-SiHA (0.4%) and control cells (0.3%). Intracellular ROS content did not show alteration in the presence of these materials, thus indicating no oxidative stress [11].

To evaluate the effects of these nanocrystalline hydroxyapatites on a cellular model more similar to the *in vivo* situation, fresh murine macrophages were obtained from the peritoneum of untreated mice and were cultured for 3 days in the presence of either nano-HA or nano-SiHA (1mg/ml) to measure cell proliferation, phagocytic activity and release of inflammatory cytokines (IL-6, TNF-α). **Figure 5A** shows a significant proliferation decrease of fresh murine macrophages induced by both hydroxyapatites ($p<0.005$). Nano-SiHA material also produce a significant decrease in phagocytosis of these cells ($p<0.005$) whose activity is not affected by nano-HA (**Figure 5B**). In spite of this decrease induced by SiHA, fresh macrophages continue phagocyting when they are in contact with this material (**Figures 6A** and **6B**). The different effect of nano-HA on RAW and fresh macrophages can be due to the higher values of phagocytosis obtained with fresh macrophages which always showed higher fluorescence values (Figure 5 B) than RAW macrophages (Figure 3B). This fact can be associated with a lower sensitivity to nano-HA of fresh macrophages although the phagocytic activity of these cells was affected by nano-SiHA.

Since the hydroxyapatite bioactivity could produce the sequestration of calcium in the extracellular medium, and taking into account that the Ca^{2+} ion plays a crucial role in cell

processes [28], Ca^{2+} levels were measured in the culture medium. **Figure 7** shows a significant Ca^{2+} decrease in the culture medium produced by both nano-HA and nano-SiHA, more pronounced with nano-SiHA, in agreement with the higher bioactivity of this material [27]. The observed sequestration of extracellular calcium can be partially responsible of the lower proliferation produced by nano-HA and nano-SiHA, as it has been described in other cell types [29]. Concerning the possible effect of extracellular calcium depletion on phagocytosis, some studies have shown that macrophages can still phagocyte in the absence of calcium through Fc receptor mediated pathways [30]. On the other hand, the changes due to depletion of extracellular calcium could be decreased *in vivo* by the dynamic flow conditions of the body fluids [31].

It is well known that interleukin 6 (IL-6) and tumor necrosis factor alpha (TNF- α) are major inflammatory cytokines and play a crucial role in infection, inflammation and stress responses. For this reason, the release of IL-6 and TNF- α by fresh mouse macrophages was measured after 3 days of treatment with these materials. **Figure 8A** shows significant increases of IL-6 induced by nano-HA ($p<0.05$) and nano-SiHA ($p<0.005$). Both materials also triggered a significant TNF-α increase (**Figure 8B**), which was more pronounced with nano-HA ($p<0.005$) than with nano-SiHA ($p<0.05$). These results evidence the early *in vitro* response of macrophages to both nanocrystalline hydroxyapatites, suggesting that, after *in vivo* implantation, these biomaterials might induce activation of the innate immune system and production of pro-inflammatory cytokines. Although further studies are needed to elucidate the long-term response of macrophages to these materials, an *in vivo* study evidenced the moderate IL-6 and IL-8 expression in bone cells and rich IL10–containing cells distribution after 8 months of hydroxyapatite implantation [32]. This fact reveals the switch of pro-inflammatory macrophage phenotype (M1) to reparative phenotype (M2) expressing high levels of IL-10 [6] and indicates the resolution of inflammatory phase at longer times.

3.3.2. Lymphocyte response to nano-HA and nano-SiHA

T lymphocytes also play an important regulatory role in the resolution of the inflammatory process through local secretion of cytokines and chemokines, many of which are known to affect macrophage polarization [6]. In order to know the nano-HA and nano-SiHA effects on T lymphocytes as specific cells involved in adaptive immune response, SR.D10 cells were cultured in the presence of these materials (1mg/ml). SR.D10 [18] is a clone obtained from the murine $CD4^+$ Th2 cell line D10.G4.1 [19] specific for Conalbumin fragment 134–146, bound to $I\text{-}A^k$ class II major histocompatibility complex molecules. SR.D10 cells provide a convenient system to test in vitro lymphocyte activation which has been largely used as a model of T cell proliferation and signalling [33,34]. These T cells have been previously used for biocompatibility testing of different bioceramics [4]. Although non-significant differences were observed on proliferation and viability of SR.D10 lymphocytes after 3 days treatment (**Figures 9A** and **9B**), a significant increase of Sub G_1 fraction, indicative of cell apoptosis, is produced by both hydroxyapatites. This effect is accompanied by significant decreases of both S and G2M fractions (**Figure 10**).

Programmed cell death (apoptosis) is a key mechanism for regulating lymphocyte number. In T lymphocytes, two major mechanisms have been described involving: a) the activation of T cell through Fas, which leads to the caspase-8 and caspase-3 induction, and b) the loss of mitochondrial integrity controlled by members of the BcL-2 family proteins [35]. Other molecules that regulate this death process include the leukocyte common antigen CD45, which has been shown to be essential for normal signaling through the T cell receptor (TCR) and for modulating signaling through cytokine receptors [50]. SR.D10 "syngeneic-reactive D10", is a variant of the murine $CD4^+$ T helper cell clone which is hyperreactive to TCR dependent and-independent stimuli. This hyperreactivity is related to the expression of several cell surface molecules involved in T cell activation as CD45 RB receptor, abundantly expressed in SR.D10 [18]. The high levels of T cell apoptosis observed in the present study could be explained by the abundant expression of this receptor that favors this death process

through Fas and TCR-induced apoptosis [36]. The presence of either nano-HA or nano-SiHA produces a significant increase of SR.D10 apoptosis probably through these mechanisms.

All these studies and previous results obtained with many different biomaterials demonstrate different cellular responses which are dependent on each biomaterial and depending on each cell type [37-39].

4. Conclusions

The *in vitro* evaluation of the early immune response to nanocrystalline hydroxyapatites evidences significant decreases of macrophage proliferation and phagocytic activity. These biomaterials also induce the production of the pro-inflammatory cytokines IL-6 and TNF-α by murine fresh macrophages and trigger apoptosis mechanisms in SR.D10 T lymphocytes. The study of the early immune response is the first step to know whether a phenotypic switch of pro-inflammatory (M1) to reparative macrophages (M2) occurs in the presence of these materials. The results obtained will be used in further studies to elucidate the long-term response of immune cells to these nanocrystalline hydroxyapatites which conditions the biomaterial success or rejection. The detection of specific macrophage markers and cytokines will allow a better understanding of the effects at longer times of these biomaterials on the equilibrium of these two distinct macrophage subsets which represents a key factor for establishing their applicability for bone Tissue Engineering.

Acknowledgements

This study was supported by research grants from Comunidad de Madrid through the project S2009/MAT-1472 and the Ministerio de Ciencia e Innovacion (MICINN) through the projects MAT2012-35556 and CSO2010-11384-E (Agening Network of Excellence). J.M. Rojo is

supported by Grant PI10/00650 from "Plan Estatal I+D+i, ISCIII-Subdirección General de Evaluación y Fomento de la Investigación, Ministerio de Economía y Competitividad (MINECO), Spain. M.C. Matesanz is greatly indebted to MICINN for the predoctoral fellowship. The authors wish to thank also to Javier Linares for technical assistance and to the staff of the Cytometry and Fluorescence Microscopy Center of the Universidad Complutense de Madrid (Spain).

References

1. Wilson CJ, Clegg RE, Leavesley DI, Pearcy MJ. Mediation of biomaterial-cell interactions by adsorbed proteins: a review. Tissue Eng 2005;11:1-18.
2. Gorbet MB, Sefton MV. Biomaterial-associated thrombosis: roles of coagulation factors, complement, platelets and leukocytes. Biomaterials 2004;25:5681-5703.
3. Smith MJ, White KL Jr, Smith DC, Bowlin GL. *In vitro* evaluations of innate and acquired immune responses to electrospun polydioxanone-elastin blends. Biomaterials 2009;30:149-159.
4. Alcaide M, Portolés P, López-Noriega A, Arcos D, Vallet-Regí M, Portolés MT. Interaction of an ordered mesoporous bioactive glass with osteoblasts, fibroblasts and lymphocytes, demonstrating its biocompatibility as a potential bone graft material. Acta Biomaterialia 2010;6:892-899.
5. Medzhitov R, Janeway CA Jr. Innate immunity. N Engl J Med 2000;343:338-344.
6. Brown BN, Ratner BD, Goodman SB, Amar S, Badylak SF. Macrophage polarization: an opportunity for improved outcomes in biomaterials and regenerative medicine. Biomaterials 2012;33:3792-3802.
7. Franz S, Rammelt S, Scharnweber D, Simon JC. Immune responses to implants: a review of the implications for the design of immunomodulatory biomaterials. Biomaterials 2011;32:6692-6709.

8. Dorozhkin SV. Bioceramics of calcium orthophosphates. Biomaterials 2010;31:1465-1485.
9. Vallet-Regí M, Arcos D. Silicon substituted hydroxyapatites. A method to upgrade calcium phosphate based implants. J Mater Chem 2005;15:1509-1516.
10. Porter AE, Patel N, Skepper JN, Best SM, Bonfield W. Comparison of *in vivo* dissolution processes in hydroxyapatite and silicon-substituted hydroxyapatite bioceramics. Biomaterials 2003;24:4609-4620.
11. Matesanz MC, Feito MJ, Ramírez-Santillán C, Lozano RM, Sánchez-Salcedo S, Arcos D, Vallet-Regí M, Portolés MT. Signaling pathways of immobilized FGF-2 on silicon-substituted hydroxyapatite. Macromol Biosci 2012;12:446-453.
12. Balamurugan A, Rebelo AHS, Lemos AF, Rocha JHG, Ventura JMG, Ferreira JMF. Suitability evaluation of sol-gel derived Si-substituted hydroxyapatite for dental and maxillofacial applications through *in vitro* osteoblasts response. Dent Mater 2008;24:1374-1380.
13. Arcos D, Rodríguez-Carvajal J, Vallet-Regí M. Silicon incorporation in hydroxyapatite obtained by controlled crystallization. Chem Mater 2004;16:2300-2308.
14. Carlisle EM. Silicon: a requirement in bone formation independent of vitamin D1. Calcif Tissue Int 1981;33:27-34.
15. Dorozhkin SV. Nanodimensional and nanocrystalline apatites and other calcium orthophosphates in biomedical engineering, biology and medicine. Materials 2009;2:1975-2045.
16. Kay MI, Young RA, Posner AS. Crystal structure of hydroxyapatite. Nature 1964;204:1050-1052.

17. Mishell BB, Shiigi JM. Preparation of mouse cell suspensions. In: Mishell BB, Shiigi JM, editors. Selected Methods in Cellular Immunology. San Francisco: WH Freeman & Co., 1980. p.1-28.

18. Ojeda G, Ronda M, Ballester S, Díez-Orejas R, Feito MJ, García-Albert L, Rojo JM, Portolés P. A hyperreactive variant of a $CD4^+$ T cell line is activated by syngeneic antigen presenting cells in the absence of antigen. Cell Immunol 1995;164:265-278.

19. Kaye J, Porcelli S, Tite J, Jones B, Janeway CA Jr. Both a monoclonal antibody and antisera specific for determinants unique to individual cloned helper T cell lines can substitute for antigen and antigen-presenting cells in the activation of T cells. J Exp Med 1983;158:836-856.

20. Robinson RA. An electron-microscopic study of the crystalline inorganic component of bone and its relationship to the organic matrix. J Bone Joint Surg Am, 1952; 34:389-476.

21. Rosengren A, Pavlovic E, Oscarsson S, Krajewski A, Ravaglioli A, Piancastelli A. Plasma protein adsorption pattern on characterized ceramic biomaterials. Biomaterials 2002;23:1237–1247.

22. Kou PM, Babensee JE. Macrophage and dendritic cell phenotypic diversity in the context of biomaterials. J Biomed Mat Res A 2011;96:239-260.

23. Scheel J, Weimans S, Thiemann A, Heisler E, Hermann M. Exposure of the murine RAW-264.7 macrophage cell line to hydroxyapatite dispersions of various composition and morphology: assessment of cytotoxicity, activation and stress response. Toxicol in Vitro 2009;23:531-538.

24. Nagata M. Inflammatory cells and oxygen radicals. Curr Drug Targets Inflamm Allergy 2005;4:503-504.

25. Vallet-Regí M, Ruiz-Hernández E. Bioceramics: from bone regeneration to cancer nanomedicine. Adv Mater 2011;23:5177-5218.

26. Thian ES, Huang J, Best SM, Barber ZH, Brooks RA, Rushton N, Bonfield W. The response of osteoblasts to nanocrystalline silicon-substituted hydroxyapatite thin films. Biomaterials 2006;27:2692-2698.

27. Pietak AM, Reid JW, Stott MJ, Sayer M. Silicon substitution in the calcium phosphate bioceramics. Biomaterials 2007;28:4023-4032.

28. Zhivotovskya B, Orreniusa S. Calcium and cell death mechanisms: a perspective from the cell death community. Cell Calcium 2011;50:211-221.

29. Dvorak MM, Siddiqua A, Ward DT, Carter DH, Dallas SL, Nemeth EF, Riccardi D. Physiological changes in extracellular calcium concentration directly control osteoblast function in the absence of calciotropic hormones. Proc Nat Acad Sci USA 2004;101:5140-5145.

30. Jesse TM, Swanson JA. Calcium spikes in activated macrophages during Fcγ receptor-mediated phagocytosis. J Leukoc Biol 2002;72: 677-684.

31. da Silva HM, Mateescu M, Damia C, Champion E, Soares G, Anselme K. Importance of dynamic culture for evaluating osteoblast activity on dense silicon substituted hydroxyapatite. Colloids Surf B: Biointerfaces 2010;80:138-144.

32. Pilmane M, Salms G, Skagers A. Characterization of molecular events in the jaw of experimental animals after different time of hydroxyapatite (HAP) implantation. Int J Oral Maxillofac Surg 2001;40:1211-1218.

33. Díez-Orejas R, Ballester S, Feito MJ, Ojeda G, Criado G, Ronda M, Portolés P, Rojo JM. Genetic and immunochemical evidence for CD4-dependent association of $p56^{lck}$ with the αβ T-cell receptor (TCR): regulation of TCR-induced activation. EMBO J 1994;13:90-99.

34. Rojo JM, Janeway CA Jr. The biologic activity of anti-T cell receptor V region monoclonal antibodies is determined by the epitope recognized. J Immunol 1988;140:1081-1088.

35. Liu Z, Dawes R, Petrova S, Beverley PCL, Tchilian EZ . CD45 regulates apoptosis in peripheral T lymphocytes. Int Immunol 2005;18:959–966.

36. Ramaswamy M, Cruz AC, Cleland SY, Deng M, Price S, Rao VK, Siegel RM. Specific elimination of effector memory $CD4^+$ T cells due to enhanced Fas signaling complex formation and association with lipid raft microdomains. Cell Death Differ 2011;18:712-720.

37. Serrano MC, Pagani R, Vallet-Regí M, Peña J, Rámila A, Izquierdo I, Portolés MT. In vitro biocompatibility assessment of poly(ε-caprolactone) films using L929 mouse fibroblast. Biomaterials 2004;25:5603-5611.

38. Alcaide M, Portolés P, López-Noriega A, Arcos D, Vallet-Regí M, Portolés MT. Interaction of an ordered mesoporous bioactive glass with osteoblasts, fibroblasts and lymphocytes demonstrates its biocompatibility as a potential bone graft material. Acta Biomater 2010;6:892-899.

39. Cicuéndez M, Portolés MT, Izquierdo-Barba I, Vallet-Regí M. New nanocomposite system with nanocrystalline apatite embedded into mesoporous bioactive glass. Chem Mater 2012;24:1100-1106.

Figure Legends

Figure 1. Experimental (circles) and calculated (solid line) powder X-ray diffraction pattern for (up) nano-HA and (down) nano-SiHA.

Figure 2. BSA adsorption profiles on nano-HA and nano-SiHA after 5 hours treatment.

Figure 3. Effects of nano-HA and nano-SiHA on proliferation (A) and phagocytosis (B) of murine RAW-264.7 macrophages after 3 days treatment. ***$p<0.005$.

Figure 4. Morphology evaluation by confocal microscopy of murine RAW-264.7 macrophages after 3 days treatment with nano-HA (B) and nano-SiHA (C). Controls without material are also included (A). Detail of RAW-264.7 cells in the presence of nano-SiHA (D).

Figure 5. Effects of nano-HA and nano-SiHA on proliferation (A) and phagocytosis (B) of murine fresh macrophages after 3 days treatment. ***$p<0.005$.

Figure 6. Morphology evaluation by confocal microscopy of phagocytosis of rabbit IgG-FITC-coated latex beads (in green) by murine fresh macrophages after 3 days treatment with nano-SiHA. A) Panoramic image. B) Detail of the macrophage phagocyting activity.

Figure 7. Effects of nano-HA and nano-SiHA on Ca^{2+} levels in the culture medium after 3 days treatment. *$p<0.05$.

Figure 8. Effects of nano-HA and nano-SiHA on IL-6 (A) and TNF-α (B) release by murine fresh macrophages after 3 days treatment. *$p<0.05$, ***$p<0.005$.

Figure 9. Effects of nano-HA and nano-SiHA on proliferation (A) and viability (B) of SR.D10 lymphocytes after 3 days treatment.

Figure 10. Effects of nano-HA and nano-SiHA on cell cycle phases of SR.D10 lymphocytes after 3 days treatment. *$p<0.05$, ***$p<0.005$.

Table I. Experimental Ca, P and Si content (% in weight) obtained by X-ray fluorescence spectroscopy. Theoretical values are indicated below in brackets.

Table II. Lattice parameters and crystallite sizes obtained from Rietveld refinements. [(a)] The values in brackets for mean crystallite size do not make reference to the measurement errors, but are an estimation of the crystal size anisotropy.

Table III. Effects of nano-HA and nano-SiHA on cell viability, apoptosis, ROS production and LDH release into the culture medium of murine RAW-264.7 macrophages after 3 days treatment.

Figure 1

Click here to download high resolution image

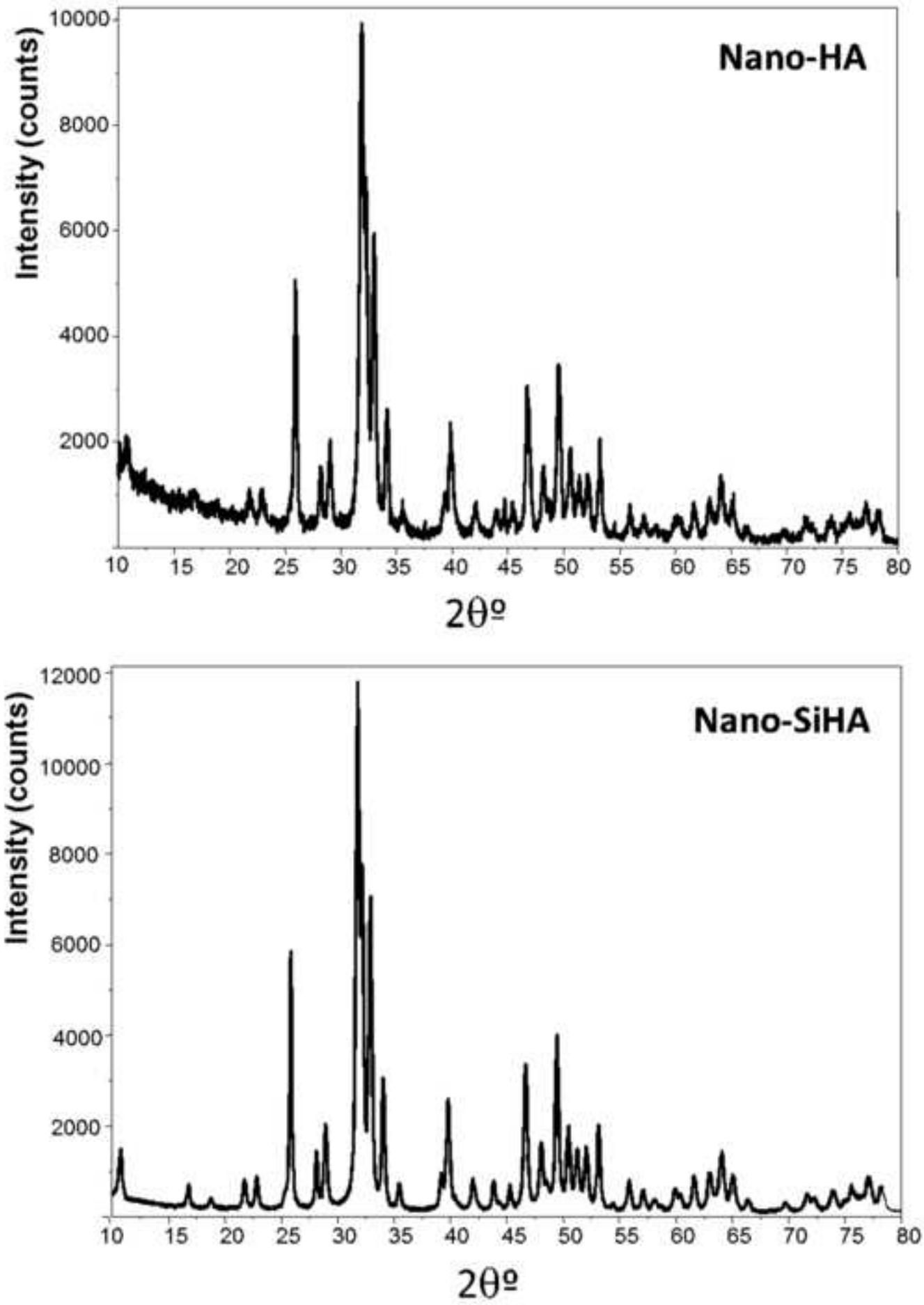

Figure 2

Click here to download high resolution image

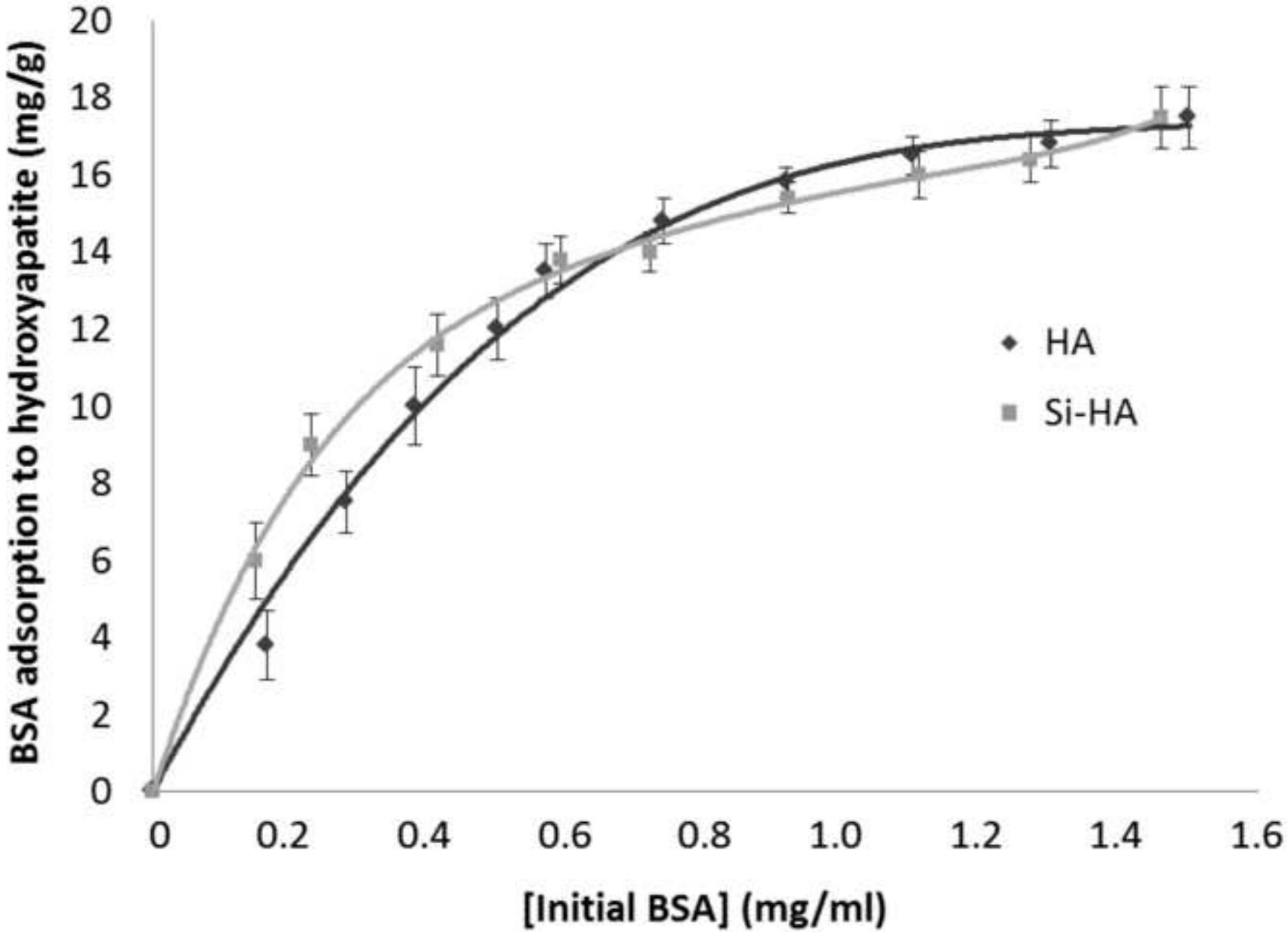

5: Figure 3

Click here to download high resolution image

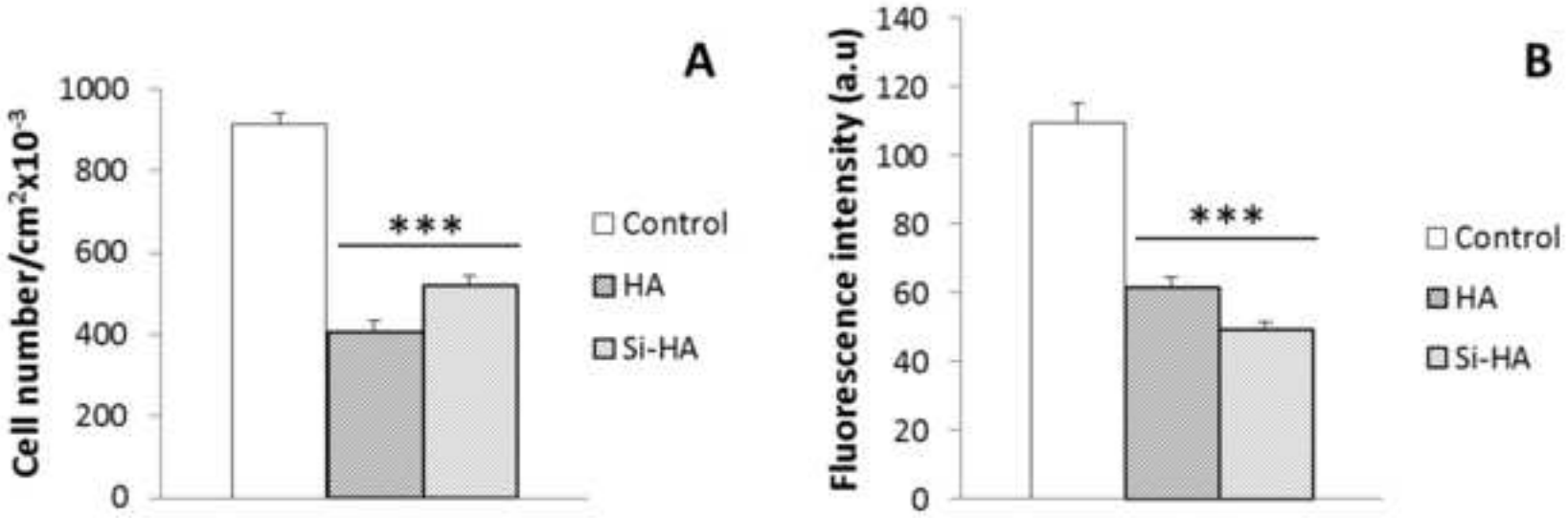

Figure 4

Click here to download high resolution image

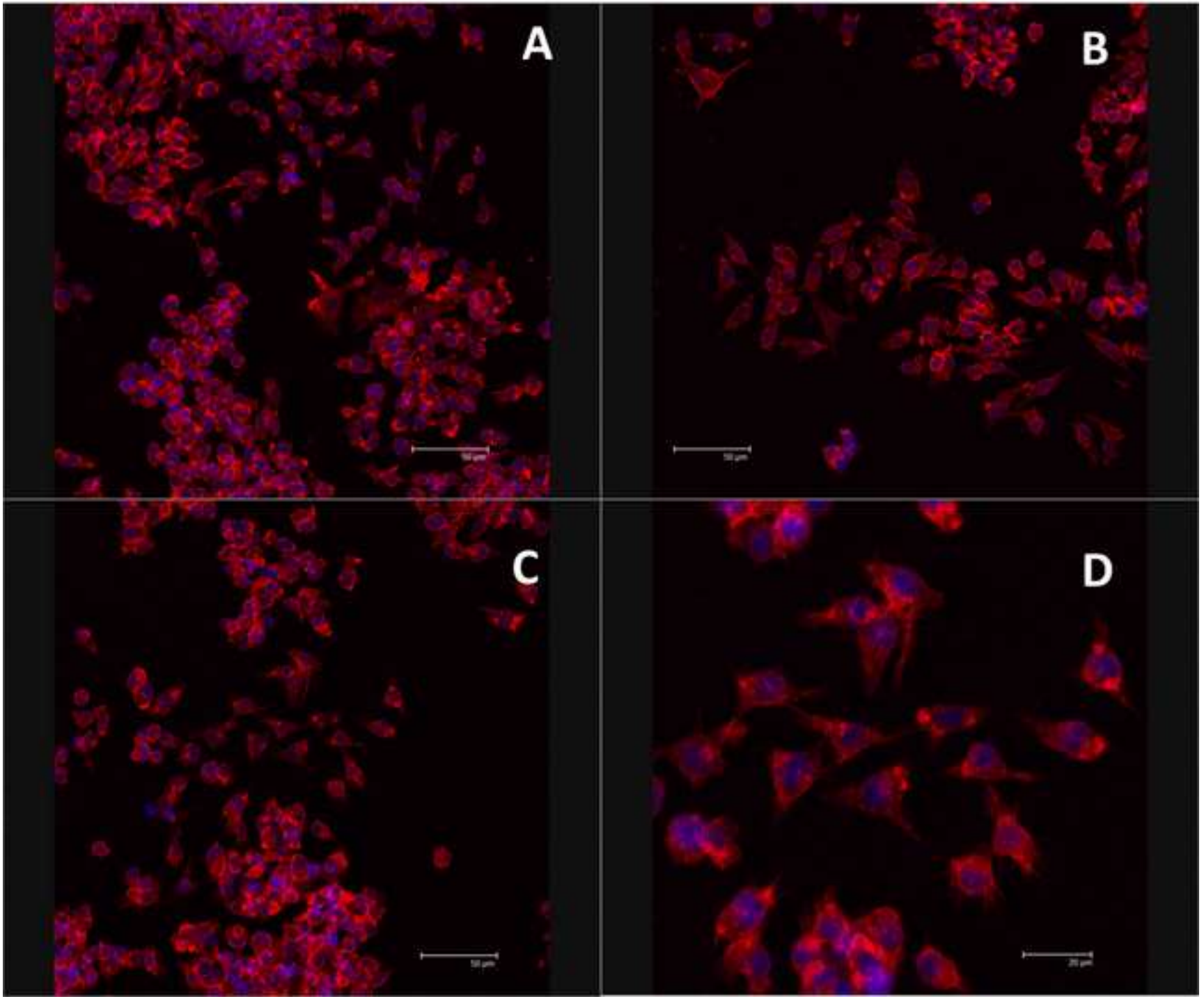

5: Figure 5

Click here to download high resolution image

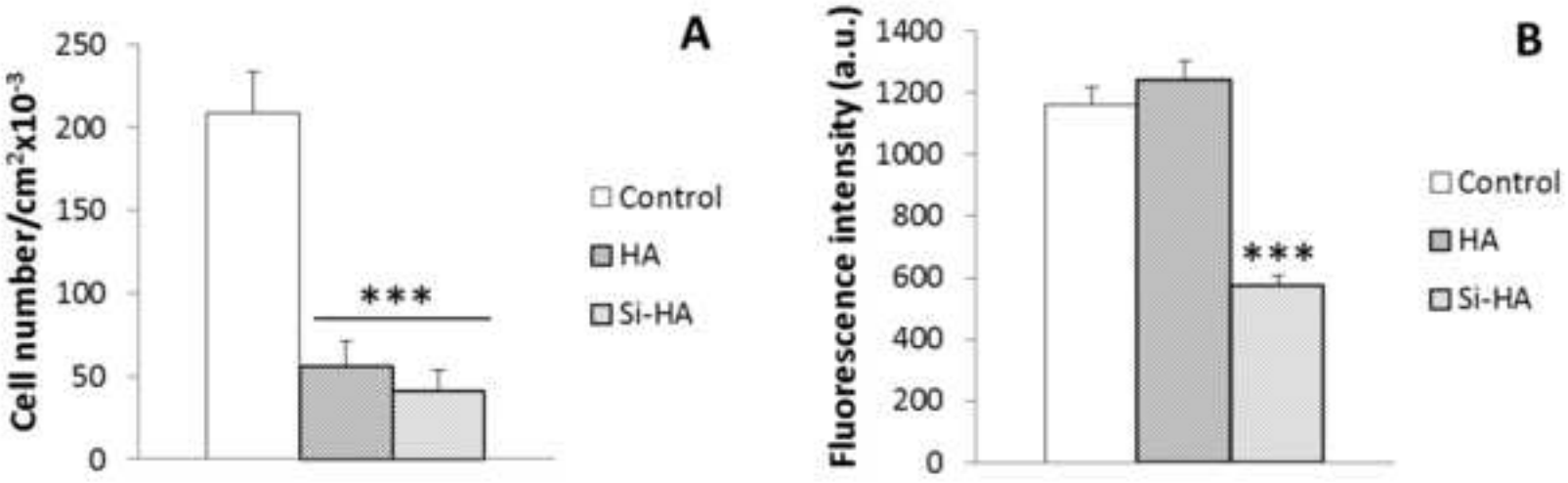

Figure 6

Click here to download high resolution image

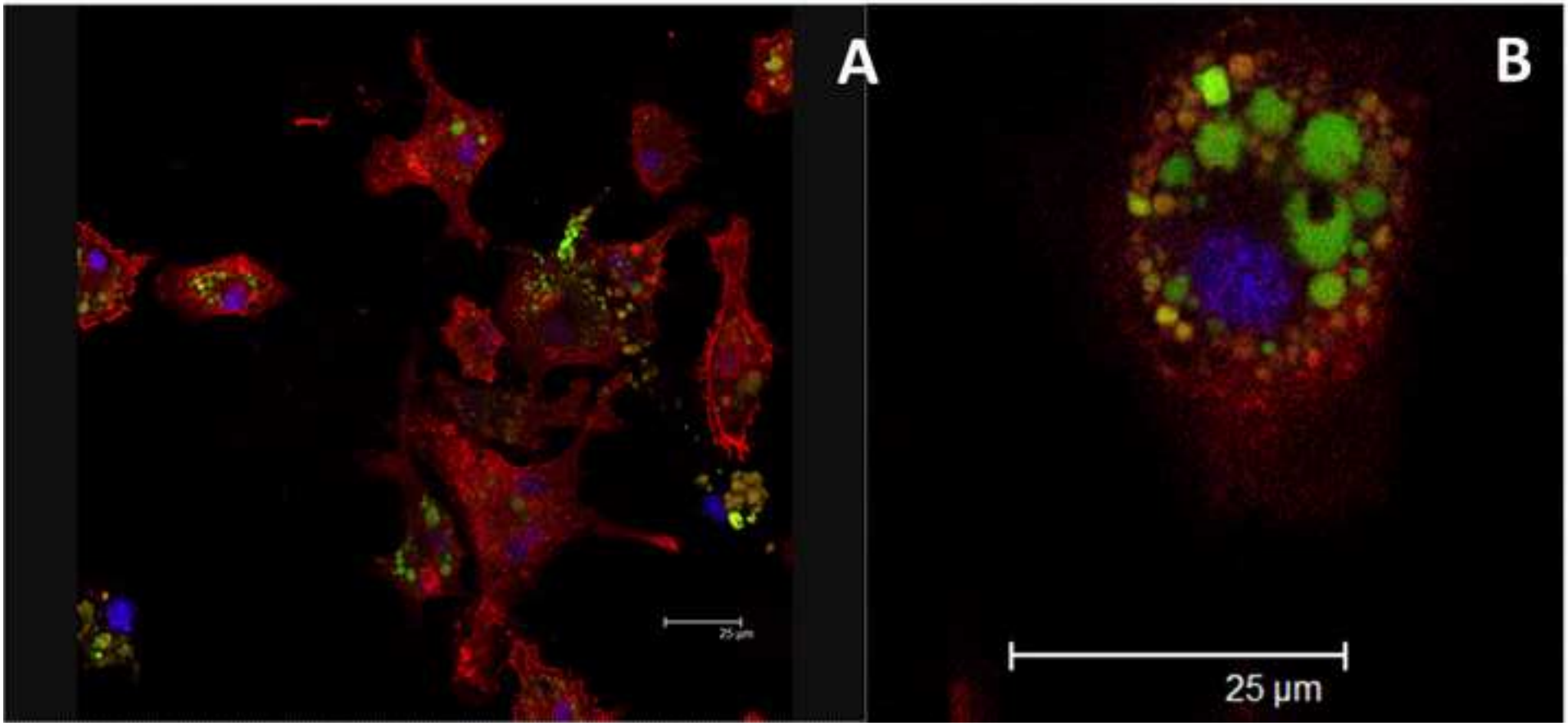

5: Figure 7
Click here to download high resolution image

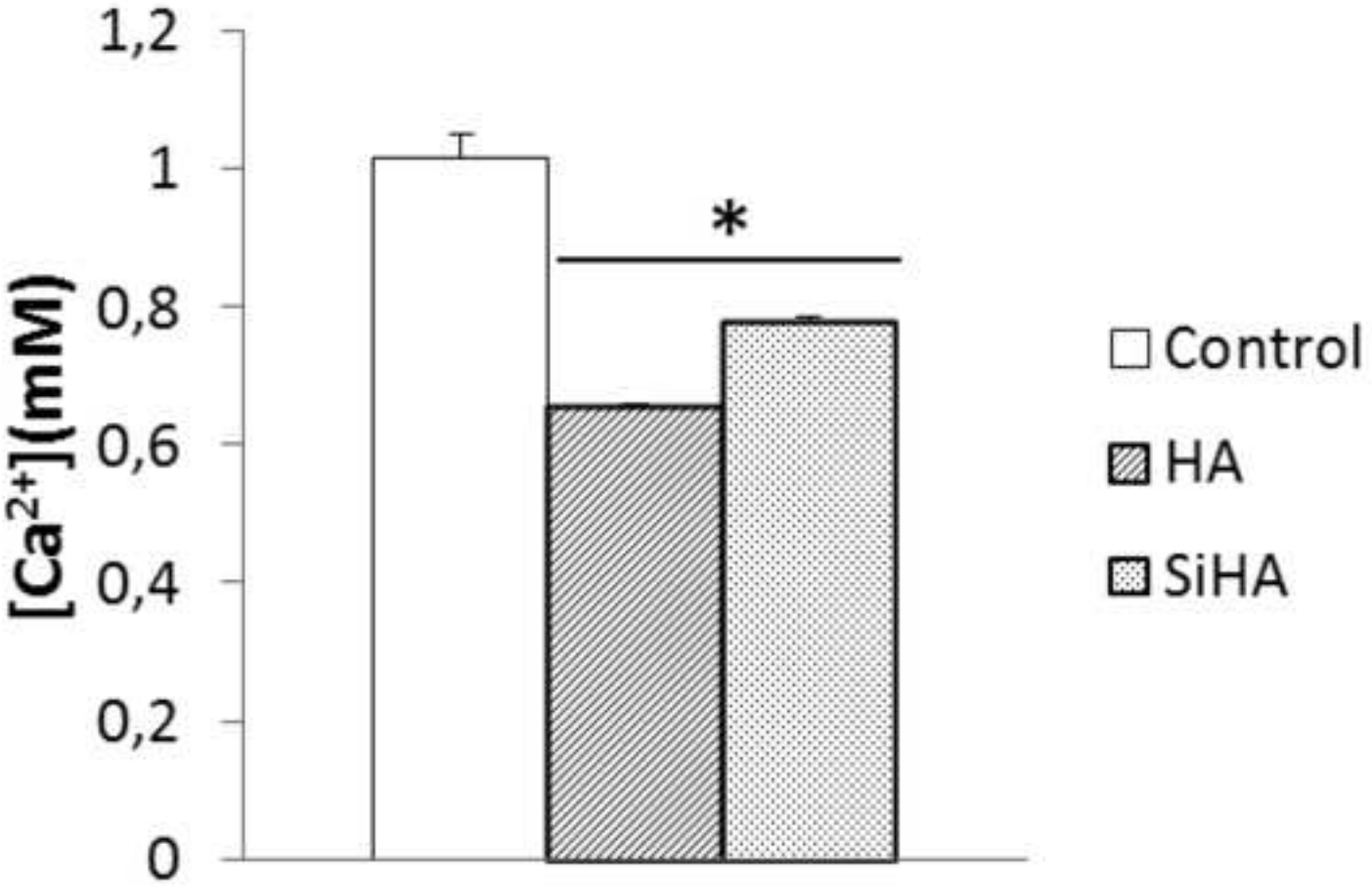

5: Figure 8
Click here to download high resolution image

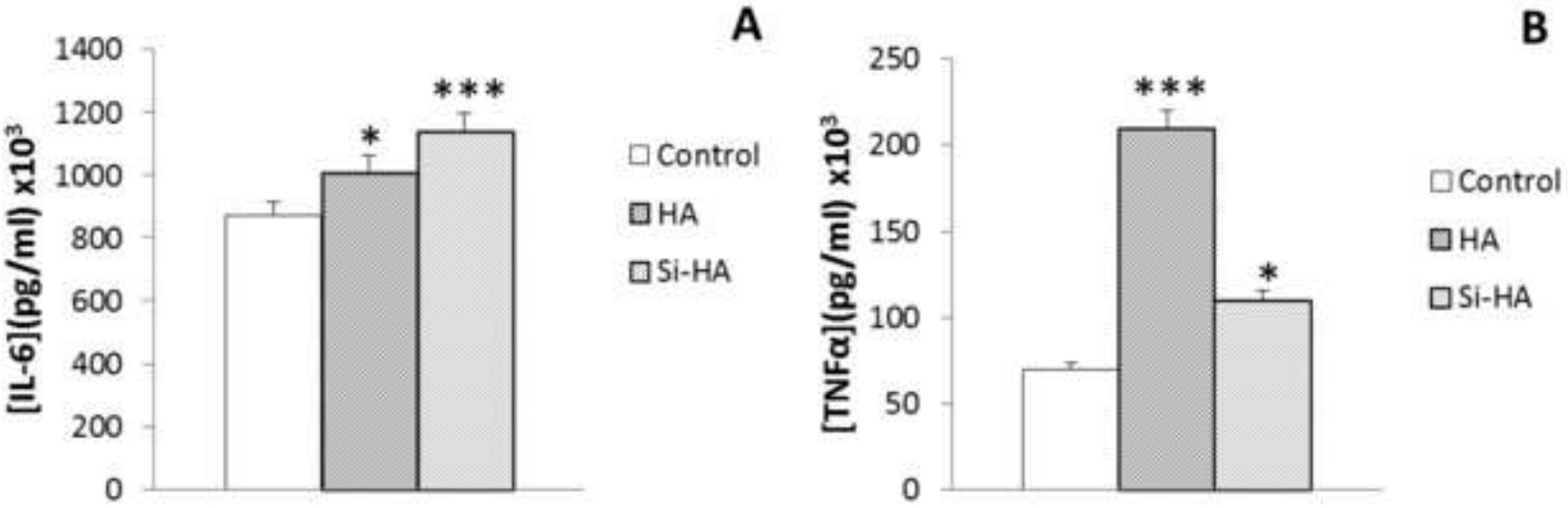

5: Figure 9
Click here to download high resolution image

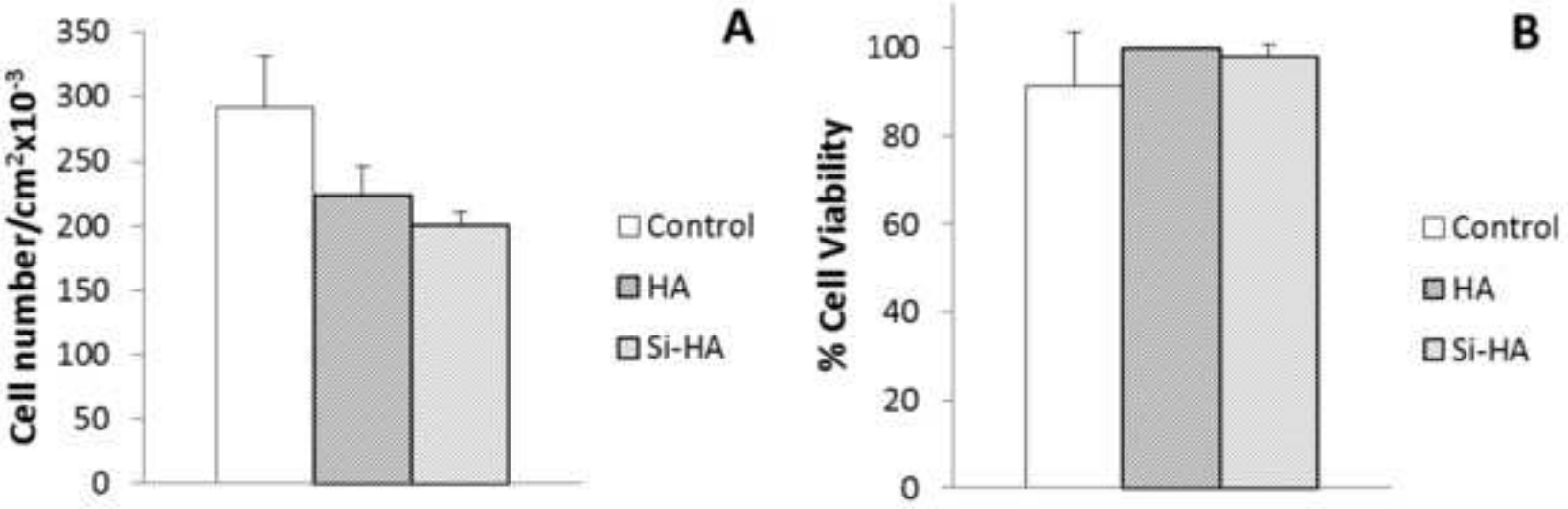

5: Figure 10

Click here to download high resolution image

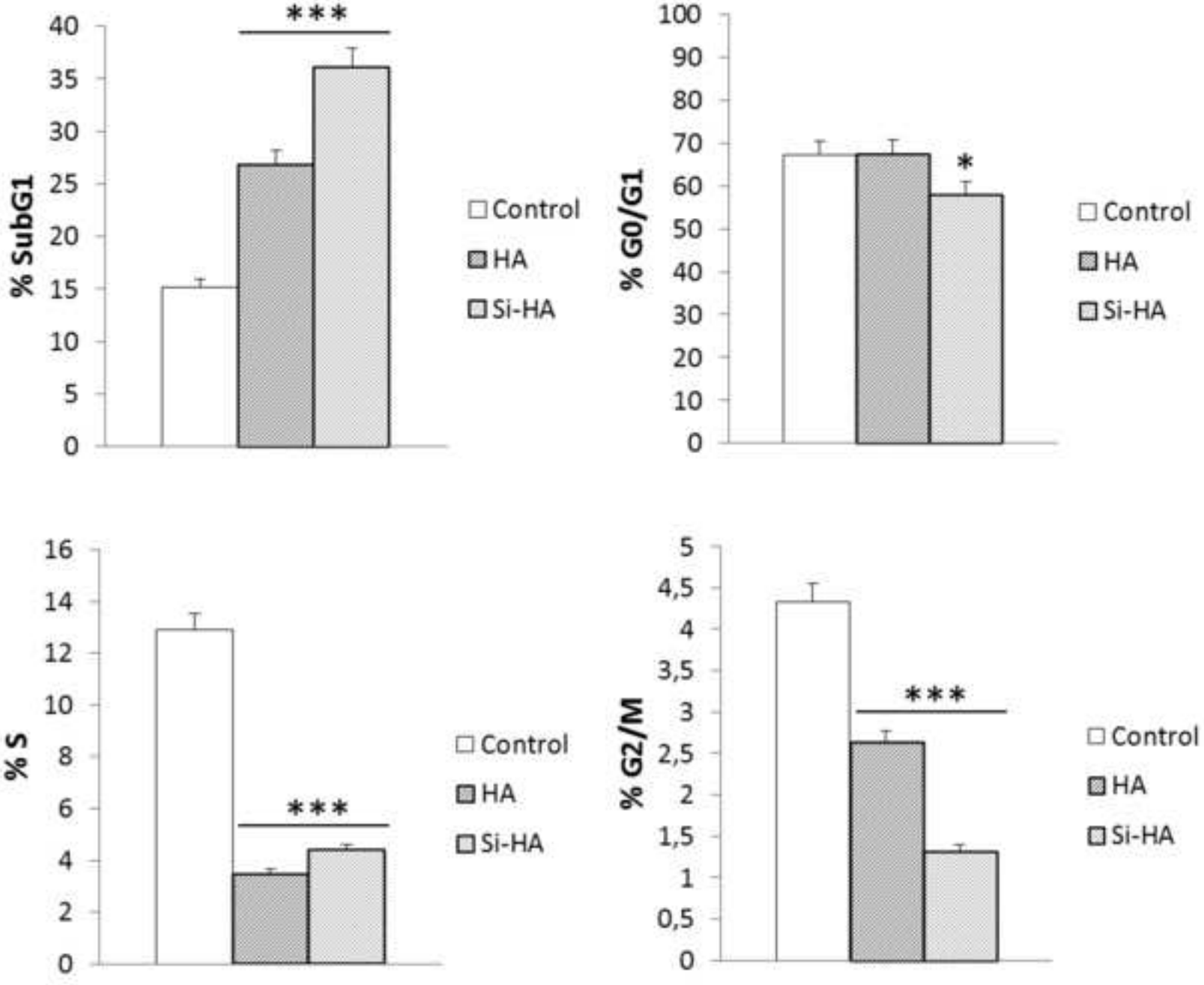

Table I
Click here to download high resolution image

Table I. Experimental Ca, P and Si content (% in weight) obtained by x-ray fluorescence spectroscopy. Theoretical values are indicated below in brackets

Sample	Ca	P	Si
Nano-HA	39.5 (39.9)	17.8 (18.5)	0.0 (0.0)
Nano-SiHA	39.2 (40.1)	17.2 (17.8)	0.6 (0.7)

Table II
Click here to download high resolution image

Table II. Lattice parameters and crystallite sizes obtained from Rietveld refinements.

Sample	Lattice parameters (Å)	Crystallite size along [1 0 0] (nm)	Crystallite size along [0 0 1] (nm)	Mean crystallite size [a] (nm)
Nano-HA	a = 9.4209 (1) c = 6.8841 (1)	27.6	48.2	30 (8)
Nano-SiHA	a = 9.4236 (1) c = 6.8875 (1)	19.1	32.9	22 (6)

[a] The values in brackets for mean crystallite size do not make reference to the measurement errors, but are an estimation of the crystal size anisotropy.

Table III
Click here to download high resolution image

Table III. Effects of nano-HA and nano-SiHA on cell viability, apoptosis, ROS production and LDH release into the culture medium of murine RAW-264.7 macrophages after 3 days treatment.

	Control	Nano-HA	Nano-SiHA
VIABILITY (%)	83.3 ± 1.8	77.1 ± 3.1	84.3 ± 0.1
APOPTOSIS (%)	2.6 ± 0.3	1.4 ± 0.1	1.9 ± 1.3
ROS (a.u.)	403.1 ± 104.0	310.8 ± 75.6	308.9 ± 105.5
LDH (U/L)	16.1 ± 2.9	25.8 ± 11.8	22.2 ± 8.2